UNIVERSITA' DELLA CALABRIA

Dipartimento di Ingegneria per l'Ambiente e il Territorio e Ingegneria Chimica

(Sede amministrativa del Corso di Dottorato)

Scuola di Dottorato in Scienze Ingegneristiche "PITAGORA"

Dottorato di Ricerca in

INGEGNERIA IDRAULICA PER L'AMBIENTE E IL TERRITORIO

CICLO

XXVIII

ACCURACY ASPECTS IN FLOOD PROPAGATION STUDIES DUE TO EARTHFILL DAM FAILURES

Settore Scientifico Disciplinare ICAR/02

Coordinatore: Prof. Ing. FRANCESCO MACCHIONE

Supervisori: Dott. Ing. PIERFRANCO COSTABILE

Dott. Ing. CARMELINA COSTANZO

Dottorando: Dott. Ing. BABAK RAZDAR

Dedication to my beloved wife and devoted dad, mom, and brother

for their endless love and support

Acknowledgements

The completion of this dissertation would not have been possible without the support and contribution of many people. I would like to thank all those who inspired and helped me throughout this journey. First and foremost, it is a great honor for me to express my deepest sincere gratitude to my supervisors, Professor Francesco Macchione, Engineer Pierfranco Costabile and Engineer Carmelina Costanzo for their support, guidance, patience, and encouragement during my PhD program of study. I have learned a great deal from their keen observations, scientific intuition, and vast knowledge base. It has been a privilege to have the opportunity to work with them.

I would like to express deep gratitude to Engineer Pierfranco Costabile for his continuous help, support, patience and kindness. Engineer Costabile was always available for my questions and gave generously of his time and knowledge along with positive encouragement. I learned a great deal from him throughout my time at LAMPIT.

I greatly appreciate Engineer Gianluca Dilorenzo as well for kindly providing the field data and sharing his input to our research.

I am deeply grateful to be surrounded by many peers and friends who have been both helpful and supportive.

I would like to special thanks to my beloved wife, Parinaz whose gave me strength along the way. Above all, I would like to express my deepest gratitude to my devoted parents Shahla and Moein, my brother Barbod for their endless support through my entire life.

ACCURACY ASPECTS IN FLOOD PROPAGATION STUDIES DUE TO EARTHFILL DAM FAILURES

Babak Razdar, Ph.D.

The University of Calabria, 2016

Supervisors:

Dott. Ing. Pierfranco Costabile

Dott. Ing. Carmelina Costanzo

Abstract

Flooding due to dam failing is one of the catastrophic disasters which might cause significant damages in the inundated area downstream of the dam. In particular, there is a need of trustworthy numerical techniques for achieving accurate computations, extended to wide areas, obtained flood mapping and, consequently, at the implementation of defensive measures. In general several key aspects are required for accurate simulations of flood phenomena which are ranging from the choice of the mathematical model and numerical schemes to be used in the flow propagation to the characterization of the topography, the roughness and all the structures which might interact with the flow patterns. Regarding general framework discussed before this thesis is devoted to discuss two aspects related to accuracy issues in dam breach studies. In the first part a suitable analytical relation for the description of reservoir have been discussed

Abstract

and the second part the influence exerted by the methods used for computing the dam breach hydrograph on the simulated maximum water levels throughout the valley downstream of a dam, has been investigated. As regards the first aspect, the influence of reservoir morphology on the peak discharge and on the shape of outflow hydrograph have been investigated in the literature. The calculation of the discharge released through the breach requires the knowledge of the water level in the reservoir. It is considerable that the reservoir morphology in computational analyses cannot be expressed exactly by an analytical formula because of natural topography of the reservoir. For this reason, the information about reservoir morphology is usually published as a detail tables or plots which each value of elevation from bottom to top has a corresponding value for lake surface and reservoir volume. However, in the cases for which there is a scarcity of data, analytical expression can be obtained by interpolation of the values of the table. Usually one of the most suitable technique for interpolation data is using polynomial function but unfortunately utilizing this function for solving the problem demand several parameters. Using power function in numerical computations of breach phenomena would be advantageous, because this function is monomial type and only one parameter needs to be estimated. In this thesis, we want to present that this approach is very accurate and suitable to represent the morphology of the reservoirs, at least for dam breach studies. To reach this aim, 97 case studies have been selected from three different

Abstract

geographical regions in the world. The results of this research have been shown that the power function is suitable to obtain an accurate fitting of the reservoir rating curve using a very limited number of surveyed elevations and volumes or areas. Furthermore in this part of the research it has been shown that two points are enough for a good fitting of the curve, or even only one if volume and surface are both available for an elevation close to normal or maximum pool. Results obtained for dam breach calculations using this equation, have the same quality of those achieved using the elevation-volume table. Moreover, this research have been shown that the exponent of power equation can be expressed by a formula which has a precise morphological meaning, as it represents the ratio between the volume which the reservoir would have if it were a cylinder with its base area and height equal to the respective maximum values of the actual reservoir, and the real volume of the reservoir. Regarding the second aspect, over the complexity of the mathematical models which have been used to predict the generation of dam breach hydrograph, it is considerable that the historical observed data of discharge peak values and typical breach features (top width, side slope and so on) have been usually utilize for model validation. Actually, the important problem which should be considered here is traditionally focused on what has been observed in the dam body, because the effects of the flood wave realized in the downstream water levels usually have been neglected. This issue seems considerable because required information for the civil protection

Abstract

and flood risk activities are represented by the consequences induced by the flood propagation on the areas downstream such as maximum water levels and maximum extent of flood-prone areas, flow velocity, front arrival times etc. The water surface data is almost never linked to the reservoir filling/emptying process which can be important information for the estimation of discharge coming from the breach, are available. Moreover, it is quite unusual to have records on the flood marks signs or other effects induced on the river bed, or on the man-made structures, downstream. For this reason finding well documented case study is one of the important part of any simulation study, especially for model validation. One of the few cases in this context is represented by the Big Bay dam, located in Lamar County, Mississippi (USA), which experienced a failure on 12 March 2004. In general analyzing the simplified models for dam breach simulation is the main purpose of this second important activity of the thesis. The simplified model have been utilized in this study, in order to identify a method that, on the basis of the results obtained in terms of simulated maximum water levels downstream, might effectively represent a preferential approach for its implementation not only in the most common propagation software but also for its integration in flood information systems and decision support systems. For the reasons explained above, attention here focuses on the parametric models, widely used for technical studies, and on the Macchione (2008) model, whose predictive ability and ease of use have been already

Abstract

mentioned. To reach this purpose both a 1-D and 2-D flood propagation modelling have been utilizing in this study. The results show that the Macchione (2008) model, without any operations of ad hoc calibration, has provided the best results in predicting computation of that event. Therefore it may be proposed as a valid alternative for parametric models, which need the estimation of some parameters that can add further uncertainties in studies like these.

Indexes

List of figures

List of tables

Intoduction

General framework

Flooding events are among the most catastrophic natural disasters that might provoke significant damages in the properties downstream and even loss of lives. In particular, there is a need of reliable numerical codes in order to carry out accurate computations, extended to wide areas, aimed at flood mapping and, consequently, at the implementation of defensive measures. Accurate simulations of these situations involve several key aspects ranging from the choice of the mathematical model and numerical schemes to be used in the flow propagation to the characterization of the topography, the roughness and all the structures which might interact with the flow patterns. Depending on the specific features of the flooding events, it might be important, especially in urbanized areas, to characterize the inlet system (Russo et al., 2015) or to describe the influence of the buildings on the flow behavior (Vojinovic et al., 2013). Simulations of flood propagation are more complex in case of the flow interacting with bridges, that often are obstructed by sediments or wood materials (Ruiz-Villanueva et al., 2014) and other floating materials or that

cannot resist the flow impacts. In this context, an important aspect is the availability of LIDAR data, adequately filtered, in order to automatically recognize structures that can interact with the flow propagation (Abdullah et al., 2012). However, the use of high-performance integrated hydrodynamic modelling systems seem to be necessary in order to exploit all the topographic information offered by LIDAR data (Liang & Smith, 2015). Further complications arise in the delimitation of flood-prone due to dam failures. In particular, the problem related to the computation of dam breach hydrograph shows more difficulties in cases of failures of earthfill dams, because of the physical phenomenon consisting in a progressive failure induced by the interaction between water and embankment. The prediction of these phenomena are gaining growing attention throughout the international hydraulic research community (see, for example: Morris et al. (2008); Xu and Zhang (2009); Pierce et al. (2010); ASCE/EWRI (2011); Peng and Zhang (2012); Duricic et al. (2013); Weiming (2013)). Several models have been proposed, in the literature, to simulate these kinds of situations. For example, in the last few years, rather complex models, based on shallow water equations over a mobile bed, have been developed by Froehlich (2002), Wang and Bowles (2006a), Faeh (2007) and Cao et al. (2011). Generally, these approaches include also a sudden removal of blocks or side collapses caused by undermining, and geotechnical or geometrical relationships are used for assessing the stability of breach sides. However, it is

important to underline that no exhaustive theory about breach morphology and breach enlargement process, based on fluid-mechanics and soil-mechanics considerations, has been proposed yet. Moreover, they have a complex mathematical structure, are based on several physical parameters and require high computational times. For this reason, several propagation software programs include specific modules for dam breaching based on the so called parametric models (Wahl, 1998). This is the case of widely used software such as HEC-RAS or NWS FLDWAV. In the parametric models, the simulated hydrograph is simulated like the emptying of a reservoir through a weir in which the bottom of the breach is lowered with time and with a preset downcutting rate (Fread and Harbaugh (1973); Singh and Snorasson (1984); Fread (1988b); Walder and O'Connor (1997)). Therefore, in such an approach, parameters such as the breach formation time and the final geometry of the breach have to be fixed a priori or estimated using empirical formulas. These relations are based on analyses of the data of historic events of dam failures, and estimate of breach width or failure time peak flow, as functions of representative quantities of the dam and the reservoir, such as the dam height or the water depth of the reservoir before failure, the storage volume, etc. (Froehlich (1995 a & b); MacDonald and Langridge-Monopolis (1984)). Wahl (2004) considered several of these methods and quantified their prediction uncertainties. One of the most important drawbacks of the parametric model is that the downcutting rate is not related to

the hydraulic flow variables but, instead, is assumed a priori similarly to the failure time. Therefore, the stopping of breach developing is generally arbitrary, because it is not at all in relationship with the physical characteristics of the flow through the breach. For this reason, it would better the use of physically-based models. However, as recalled above, more complicated models need several parameters and, therefore, should be used carefully only by experts. For example, in the technical manual of NWS FLDWAV (1998) it is reported: "The BREACH model has not been directly incorporated into FLDWAV to discourage its indiscriminate use, since it should be used judiciously and with caution". In order to avoid the drawbacks associated with the use of more complex physically-based models and the physical inconsistencies of the parametric models, a possible alternative choice is the application of simplified physically-based models. In general, they take into account the eroding flow capacity (Broich (2002); Franca and Almeida (2004); Fread (1989); Hassan et al. (2002); Macchione (1986, 1989 & 2008); Macchione and Rino (2008); Rozov (2003); Singh and Quiroga (1988); Singh and Scarlatos (1988); Tinney and Hsu (1961)), which can be expressed as a function of the mean shear stress or a function of the average flow velocity on the breach. Among the models belonging to this category, the dam-breach model proposed by Macchione (2008) predicts, in a simple but physically based manner, not only the peak discharge but also the whole outflow hydrograph and breach development. The

model considers the following issues: the geometry of the embankment, the shape of the reservoir, the shape of the breach and the hydraulic characteristics of the flow through the breach and its erosive capacity. The model needs only one calibration parameter and can be easily applied to real cases.

Scope of the thesis

Within the framework discussed so far, two aspects are discussed in this thesis both of them related to accuracy issues in dam breach studies: a suitable analytical relation for the description of reservoir morphology and the influence exerted by the methods used for computing the dam breach hydrograph on the simulated maximum water levels throughout the valley downstream of a dam. As regards the first aspect, several studies in the literature showed the influence of reservoir morphology on the peak discharge and on the shape of outflow hydrograph. Almost all simplified physically based models contain an equation describing the emptying of the reservoir due to the discharge Q_b released through the breach or through the outlets and the filling due to the possible inflow Q_{in} during a dam breaching event. The calculation of the discharge released through the breach requires the knowledge of the water level in the reservoir. Since the reservoirs have a natural topography, their geometry cannot be expressed exactly by an analytical formula. For this reason, usually detailed tables are considered for this purpose, where each value of elevation from bottom to top has a

corresponding value for lake surface and reservoir volume. These tables, very often, are plotted and the graphs are known as elevation-volume or elevation-area curves. However, in the cases for which there is a scarcity of data, we have to interpolate the values of the table to obtain an analytical expression. Therefore, it is necessary to give an equation that describes the relation between the volume W stored in the reservoir and the corresponding elevation h. Usually a polynomial function is the most suitable one, but unfortunately it requires the estimation of several parameters and this may result in some difficulties in the studies of flood control reservoirs or dam breach aimed at giving generalized solutions based on a number of representative parameters. As an example, if one wishes to develop the hydrograph computations using a non dimensional formulation, it is essential to reduce the number of parameters as much as possible. In this context the use of a polynomial function in the elevation-volume curve is not feasible. For this purpose, if applicable, it would be advantageous to express the reservoir rating curve, also called elevation-volume curve, using the power function, because this has the advantage of being a monomial function and only one parameter needs to be estimated. This expression has been already used in the past by Marone (1971), Michels (1977), Macchione (1986, 1989 & 2008), Macchione and Rino (2008) and De Lorenzo and Macchione (2011 & 2014), which used the power function in dam breach modelling for the calculation of flood hydrograph and peak discharge. However, some authors

considered the use of this kind of expression an approximate approach (ASCE/EWRI, 2011). In this thesis, we want to show that this approach is very accurate and suitable to represent the morphology of the reservoirs, at least for dam breach studies. As a consequence we will show that its use in numerical modelling does not affect the accuracy of calculations. This will be demonstrated by analysing the suitability of the power function as an interpolating equation for reservoirs located in three different regions of the world, in order to verify the applicability of the function for various geological and geomorphological contexts. Moreover, a clear morphological meaning of the exponent of the power function will be provided and discussed.

Regarding the second aspect, it should be observed that independently from the complexity of the mathematical model used for the generation of dam breach hydrograph, it is important to observe that the model validation is usually carried out by reproducing historical observed data of discharge peak values and typical breach features (top width, side slope and so on). Actually, attention is traditionally focused on what has been observed in the dam body, neglecting the effects that the flood wave had on the downstream water levels. This issue does not seem to be unimportant because the relevant elements for the civil protection and flood risk activities are represented by the consequences induced by the flood propagation on the areas downstream such as maximum water levels and maximum extent of flood-prone areas, flow velocity, front arrival times etc. In

the technical literature there is a lack of papers that focus on the influence exerted by the method used for computing the dam breach hydrograph on the flood hazard and, in particular, on the simulated maximum water levels. This operation seems to be very important for scientific purposes and, in any case, should be essential for selecting a specific computing module, to be implemented in the commercial propagation software, able to balance the need for a reasonable physical description of the phenomenon and, at the same time, limiting as much as possible the maximum number of parameters that the user should estimate to run the model. In particular, this last issue gained importance in the context of the reduction of the entire modelling uncertainty, ranging from the generation to the propagation of flood events. The lack of specific studies aimed at clarifying the issues described above is somewhat expected because it is quite unusual to have well-documented historical events for both the breach generation and the water marks downstream. In particular, the breach information is quite limited to its final dimensions and, sometimes, to an estimation of the evolution time. The water surface data is almost never linked to the reservoir emptying which can be important information for the estimation of discharge coming from the breach, are available. Moreover, it is quite unusual to have records on the flood marks signs or other effects induced on the river bed, or on the man-made structures, downstream. For this reason, any time it is possible to have well-documented test cases, these are extremely useful for model validation. One of

the few cases in this context is represented by the Big Bay dam, located in Lamar County, Mississippi (USA), which experienced a failure on 12 March 2004. The main purpose of this second important activity of the thesis is the analysis of simplified models for dam breach simulation, in order to identify a method that, on the basis of the results obtained in terms of simulated maximum water levels downstream, might effectively represent a preferential approach for its implementation not only in the most common propagation software but also for its integration in flood information systems and decision support systems.

Chapter 1

State of the art on dam breach modeling and reservoir morphology

1.1 Reservoir morphology in dam breach modelling

Almost all simplified physically based models contain an equation describing the emptying of the reservoir due to the discharge Q_{in} released through the breach or through the outlets and the filling due to the possible inflow Q_{in} during a dam breaching event. Several authors showed the influence of reservoir morphology on the peak discharge and on the shape of outflow hydrograph. The calculation of the discharge released through the breach requires the knowledge of the water level in the reservoir, therefore the equation describing the increase or decrease of water level and volume stored in the reservoir should contain a mathematical relation linking the volume or lake area with elevation. For this reason, it is necessary to give an equation that describes the relation between the volume W stored in the reservoir and the corresponding elevation h. Note that the derivative of W with respect to h is the water surface S_a:

$$\frac{dW}{dh} = S_a(h) \tag{1.1}$$

In some cases the authors (Broich, 2002; Peviani, 1999; Ponce & Tsivoglou, 1981; Singh & Quiroga, 1987; Visser, 1998) do not explicitly highlight which function should be used. Without detailed information, it can be argued that the authors leave the users free to adopt an analytical function for $S_a(h)$ or to insert a table with lake area values and the corresponding elevations. However, the last option likely requires the use of a linear interpolation to get all the possible values from those known in the table. In ASCE/EWRI (2011) the authors show a table with a review of the simplified models available in literature. For many models, the authors explicitly say that the model uses a simplified law for the volume-elevation curve. Singh and Scarlatos (1988) used a simplified approach since the average surface is given by the ratio between the volume W and elevation h, and this is equivalent to the assumption of a reservoir with vertical walls. Walder and O'Connor (1997) used the following equation:

$$\frac{W(t)}{W(t=0)} = \left(\frac{Z(t)}{Z(t=0)} \right)^m \tag{1.2}$$

which is completely equivalent to Eq. (1.1) as long as $W_0 = W(t=0) / Z(t=0)^m$. Rozov (2003) assumed a "V-Shaped" reservoir, Franca and Almeida (2004) assumed a reservoir with a rectangular base and vertical walls. However, according to them, the model can have a more accurate representation of the reservoir by giving the area as a function of elevation. Tsakiris and Spiliotis

(2013) assumed that the reservoir capacity is proportional to the water depth raised to 3 m. The model NWS-BREACH by Fread (1989) explicitly requires at least 2 and up to 8 points to be known for the function S_a *(h)*. Loukola and Huokona (1998) explicitly say that the shape of the reservoir should be described by a "volume or surface area versus elevation table". Ponce and Tsivoglou (1981); Peviani (1999); Broich (2002) for DEICH-P model and Visser (1998) for BRES model do not explain how the relation between volume or area and elevation should be expressed, but the values can always be taken from a table and linearly interpolated as clarified by Hanson et al. (2005), who for the SIMBA model explicitly say that "...volume is interpolated linearly from tabular input of an elevation-volume table for the reservoir". Finally, a different equation has been presented by Mohammadzadeh-Habili et al. (2009). The authors assume that the relation between elevation and volume or area can be represented by a modified exponential equation:

$$W = W_{\max}\left(e^{\ln(2)\frac{z}{z_{\max}}} - 1\right)^{1/N} \tag{1.3}$$

The authors state that Eq. (1.3) allows us to describe better the deviation of the points (Z, W) of a reservoir volume table, from the linear law in a log-log plot. The reservoir coefficient N can be computed by minimizing the sum of square

errors (SSE) or by lake area S_{max} and volume W_{max} at elevation Z_{max} using:

$$N = 2\ln 2\frac{V_{\max}}{S_{\max}Z_{\max}} \tag{1.4}$$

However, Eq. (1.3) shows poorer performance than the power equation proposed in this research.

Chapter 2

The Macchione (2008) model

2.1 State of the art on dam breach modeling

As it is well-known, the failure mechanism of an earth dam is progressive, and its spatial and temporal development is greatly influenced by the interaction of the flow and the embankment, which should be included in any hydrograph prediction. The hydrodynamic and mechanical aspects are particularly hard to understand for artificial structures, earthen dams built with compacted materials, with systems of internal zoning ranging from simple to quite complex. During last decades, significant experimental studies have been considered, such as laboratory tests on noncohesive embankments (Coleman et al., 2002; Russo et al., 2015). In the context of the Investigation of Extreme Flood Processes and Uncertainty (IMPACT, 2005) project, experimental data were collected from field and laboratory tests. In this project, large scale tests related to noncohesive and cohesive embankment failures were considered; the analyzed embankments included homogeneous and composite (e.g., core and outer layer) structures. The

tests highlighted a number of processes generally neglected by numerical models. These comprise modeling of the critical flow control p3oint through the breach, breach dimensions, collapsing, and head cut processes (IMPACT, 2005). Historically, it has been observed (Johnson & Illes, 1976; MacDonald & Langridge-Monopolis, 1984) that overtopping triggers an erosion process at a weak point at the top of the embankment. During enlargement process, an approximately triangular cut is initially created that, with the evolution of the phenomenon, becomes bigger and bigger until the bottom of the breach reaches the natural ground base of the dam, which is usually less erodible than the dam body. Afterwards, the sides of the breach are eroded and the breach section looks like a trapezoidal-shaped section. The extent of this lateral erosion is influenced by the erodibility of the dam body, the shape of the reservoir, and the water volume stored; the maximum contour of the breach can reach the abutments of the embankment. In any case, the breaches dimensions are always considerable, with top widths up to hundreds of meters. During piping process the embankment is eroded by the flow through a hole inside the body until the part of the dam body above it collapses into the hole. After this step a breach is formed and the development of the process is similar to the breach enlargement due to the overtopping case, described above. It should be observed that the flow passing through the hole caused by the piping is much smaller than that flowing out of the breach after the collapse of the top of the dam above it. For this reason,

,mathematical modeling aimed at the computation of the outflow hydrograph due to dam breaching can neglect the simulation of the progression of the tunnel and begin the calculation from an initial breach whose bottom is lower than the initial level of the free surface of the water in the reservoir. The similarity of the dam breach development due to piping and overtopping has been investigated by Johnson and Illes (1976). The dynamics of the dam breaching due to piping is well-documented in the case of the Teton Dam failure (Chadwick et al., 1976). The breaching events generated an outflow hydrograph whose peak discharge value was much greater than what could have followed a hydrological event in the river, rare as that might be, but of a much lower value than that which would have occurred if the breach had been produced instantly. In the case of the Teton Dam failure, for example, a value of about 50,000 m^3/s was obtained (Balloffet & Scheffler, 1982). Dam-breach models can be grouped under the hydraulic schematizations on which they are based (Macchione, 1993, 2000). For predicting the hydrograph, the simplest approach is to simulate the emptying of a reservoir through a weir for the outflow generation. The bottom of the breach is lowered with time and with a constant downcutting rate, the value of which is deduced from observations (Fread, 1988b; Fread & Harbaugh, 1973; Singh & Snorasson, 1984; Walder & O'Connor, 1997). The methods based on the above approach are called "parametric models" (Wahl, 1998). A more realistic approach should considers the eroding flow capacity (Franca & Almeida, 2004;

Fread, 1989; Macchione, 1986, 1989; Rozov, 2003; Singh & Quiroga, 1988; Singh & Scarlatos, 1988; Tinney & Hsu, 1961), that can be represented as a function of the mean shear stress or a function of the average flow velocity on the breach. Methods of this type are called "physically based methods". Besides models that consider the breach as a weir, other physically based models have been developed in the literature that consider the breach as a weir located at the top of a geometrically regular erodible channel (Giuseppetti & Molinaro, 1989; Singh & Scarlatos, 1989). More accurate schemes, based on the De Saint-Venant equations for the description of the flow behavior, have been also proposed in the literature (Benoist & Nicollet, 1983; Costabile et al., 2004; Macchione & Sirangelo, 1989; Ponce & Tsivoglou, 1981). The spatial and temporal development of the breach is simulated by calculating the erosion according to the sediment continuity equation. As regards the morphological evolution of the breach, many of the above-mentioned models assume a continuous development induced by the hydrodynamic action of the flow and, for the calculation of the transport rate, refer to the classical sediment transport formulas. Sometimes, the instability of breach side portions has been somewhat take into account using stability analyses based on the principles of soil mechanics (Fread, 1988a; Mohamed et al., 2002; Singh, 1996). An extensive review of dam-breach modeling can be found in Singh (1996). Statistical models consider data of historic events of dam failures, and evaluate the peak flow or breach width or

failure time, as functions of a number of characteristic quantities of the dam and the reservoir, such as the height of the dam or the water depth of the reservoir before failure, the storage volume, etc. (Froehlich, 1995a, 1995b; MacDonald & Langridge-Monopolis, 1984). Wahl (2004) analyzed several of these techniques and provide a quantification of the associated prediction.

2.2 General features of the Macchione (2008) model

Macchione (2008) proposed a physically based model that can calculate, in a simple manner, not only the peak discharge but also the entire outflow hydrograph and the breach gradual growth. The main aspects involved in the dam breach process have been taken into account by this model: the geometry of the embankment, the shape of the reservoir, the hydraulic characteristics of the flow through the breach and its erosive capacity, and the shape of the breach. The model needs some input parameters such as: the level-reservoir volume curve, the height of the dam, the initial surface level in the reservoir, the crest width of the embankment, and the dam side slopes. The model can provide the flood wave hydrograph and the temporal evolution of the breach. Furthermore, the model needs only one calibration parameter and can be easily applied to real cases.

2.2.1 Assumptions and governing equations of the Macchione (2008) model

In the Macchione (2008) model, the breach cross-section is assumed to develop, at first, in a vertical direction with a triangular shape until its lower vertex reaches the base of the dam. Further progression of the breach leads to an enlargement due to erosion of the sides alone. Recorded historical observations point out a trapezoidal shape for the final geometry of the breach. However it cannot be assumed a priori that the breach sides had the same slope during the process of breach enlargement. The final (horizontal:vertical) values of the slopes are probably greater than those during the phenomenon, due to the possible collapse of part of the embankment that could have taken place some time after the emptying of the reservoir. In fact recent experimental observations point out that the breach side walls are near vertical during the erosion process (IMPACT, 2005). Therefore, as will be explained in more detail in the following section, low values of (horizontal:vertical) breach side slopes were assumed, in order to have near vertical side walls, and these were assumed to be constant for the whole duration of the phenomenon. Referring to the sketch of Fig. 1, the area A_b of the breach section is:

$$A_b = (Z_M - Y)^2 \tan\beta \tag{2.1}$$

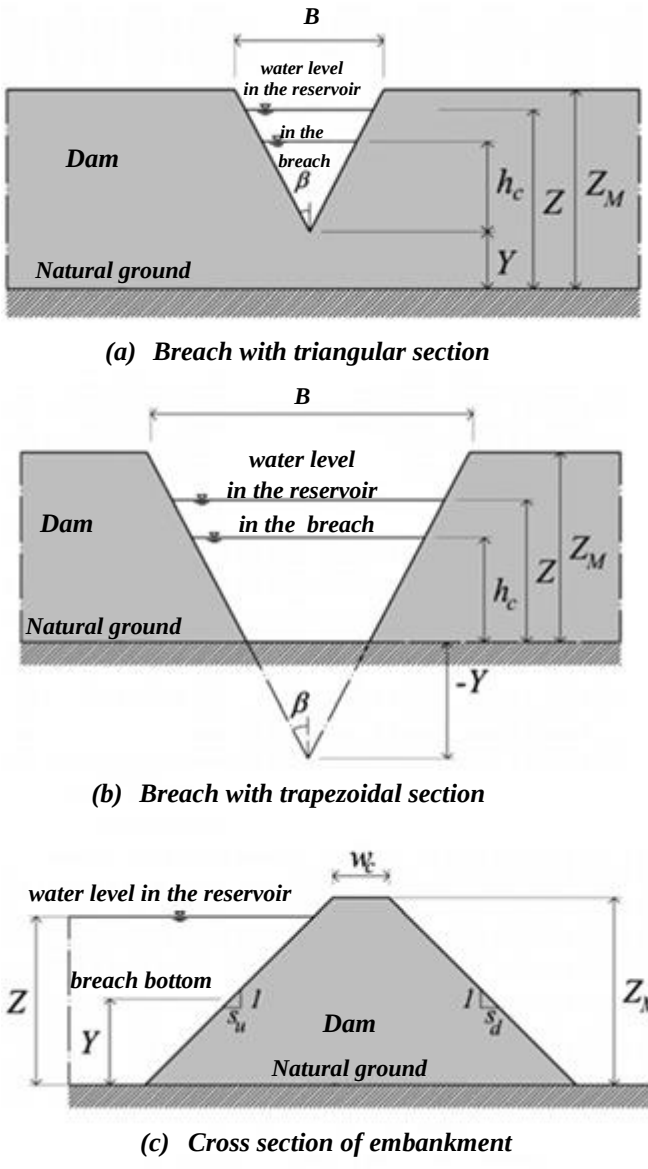

(a) Breach with triangular section

(b) Breach with trapezoidal section

(c) Cross section of embankment

Figure 1. Definition sketch of breach section

in which Z_m indicates the height of the dam; Y= vertical distance between the vertex of the triangular breach and the base of the dam; and β =angle that the sides of the breach form with the vertical. For the trapezoidal breach A_b is:

$$A_b = (Z_M - 2Y)Z_M \tan\beta \tag{2.2}$$

in which $Y(<0)$ now indicates the difference in elevation between the intersection point of the lengthened sides of the breach and the base of the dam. In the model of Macchione (2008) the transport capacity is assumed proportional to the 3/2 power of mean shear stress $\tau(N/m^2)$, (as in the Meyer-Peter and Mueller formula, if the critical shear stress is negligible in comparison with τ). Therefore, the following equation for the volumetric sediment load per unit width, q_s, has been used (Macchione, 1986, 1989):

$$q_s = k_0 \tau^{3/2} \tag{2.3}$$

where the coefficient $k_0(m^5 s^{-1} N^{-3/2})$ depends on the characteristics of the material and on the conditions in which the erosion occurs, and will be achieved through an overall calibration parameter of the model. Assuming that the eroded material below the water line is redistributed along the entire length of the sides of the breach (Cunge et al., 1980), the breach evolution process can be described by the following equation:

$$dA_b.l = c.q_s.dt \tag{2.4}$$

in which c = erodible wetted perimeter; and l = mean length of the breach.

Since $$\frac{dA_b}{dt} = \frac{dA_b}{dY}\frac{dY}{dt}$$

Eq. (2.4) can be rewritten as:

$$\frac{dY}{dt} = cq_s\left(\frac{dA_b}{dY}\right)^{-1} l^{-1} \tag{2.5}$$

The mean shear stress is expressed by the following equation:

$$\tau = \gamma RS \tag{2.6}$$

in which γ = specific weight of the water; R = hydraulic radius; and S = friction slope.

In this model, S is expressed through the Strickler equation (2.7):

$$S = \frac{V^2}{K_s^2 R^{4/3}} \tag{2.7}$$

where V = flow velocity; and K_s roughness coefficient. The model takes into account the breach as a throat through which critical flow conditions are expected (Macchione, 1986, 1989). This idea has been recently confirmed by the experimental observations of Chanson (2004), according to which "the total head is basically constant from the inlet lip to the throat, the flow is streamlined, and the flow conditions are near critical." Assuming the occurrence of critical flow through the breach, the erodible wetted perimeter c can be expressed as:

$$c = \frac{2h_c}{\cos\beta} \tag{2.8}$$

in which h_c = critical depth.

Taking into account Eqs. (2.6) – (2.8), Eq. (2.5) can be written as follows:

$$\frac{dY}{dt} = v_e \frac{2h_c}{\cos\beta} \frac{V^3}{g^{3/2} R^{1/2}} \left(\frac{dA_b}{dY}\right)^{-1} l^{-1} \tag{2.9}$$

where g = acceleration due to gravity and

$$v_e = \frac{k_0}{k_s^3} (\gamma g)^{3/2} \tag{2.10}$$

The expressions for R, V, h_c, dA_b/dY and l as functions of Z and Y are given in Table 1; in the expressions of parameters of l, S_u and S_d indicate the upstream and downstream embankment slopes and the parameter of W_c indicate crest width of the embankment. The variable v_e represents a characteristic velocity that affects the erosion velocity dY/dt; hydraulic and geometric conditions being equal, the velocity of erosion is proportional to velocity v_e. The values of v_e depends on coefficient k_0 of the volumetric sediment load equation [Eq. (2.3)] and on the Strickler coefficient K_s. It should be estimated by calibration through experimental tests or past failure events. In the study of Macchione (2008) the average value of v_e= 0.0698 m/s has been selected from the range of 0.0453–0.1022 m/s which obtained from applying the outlier-exclusion algorithm which suggested by Wahl (2004). The figures 2 and 3 show the comparison between the observed values of peak discharge and final average breach width with prediction results of the model of Macchione (2008) in predictive mode with applying average value of v_e= 0.0698 m/s. The results of this study have been

shown that the mean parameter of v_e= 0.0698 m/s described very well the 12 considered dam breach case studies.

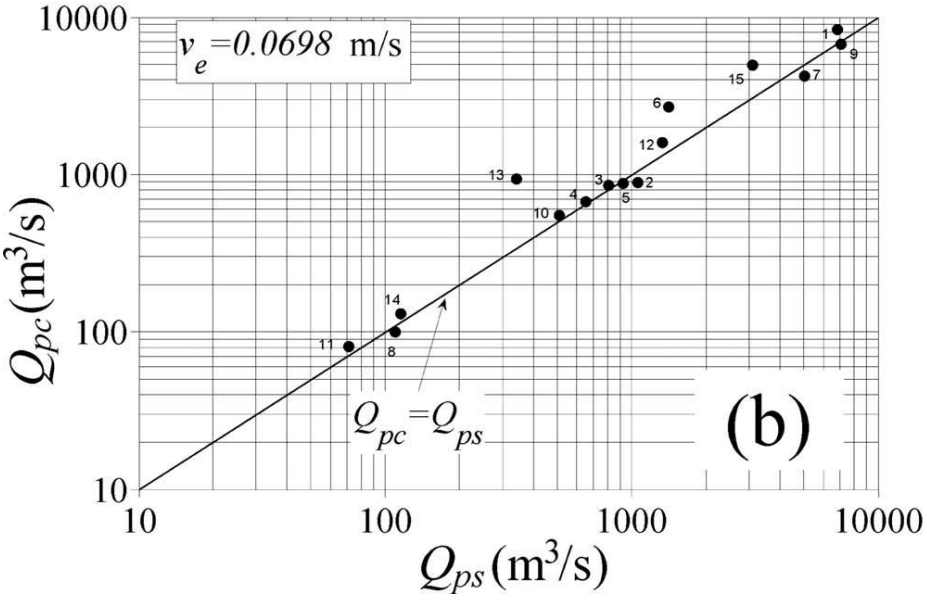

Figure 2. Predicted peak discharge Qpc versus observed peak discharge Qps for earthen dam failures which considered in the study of Macchione (2008) with ve=0.0698 m/s

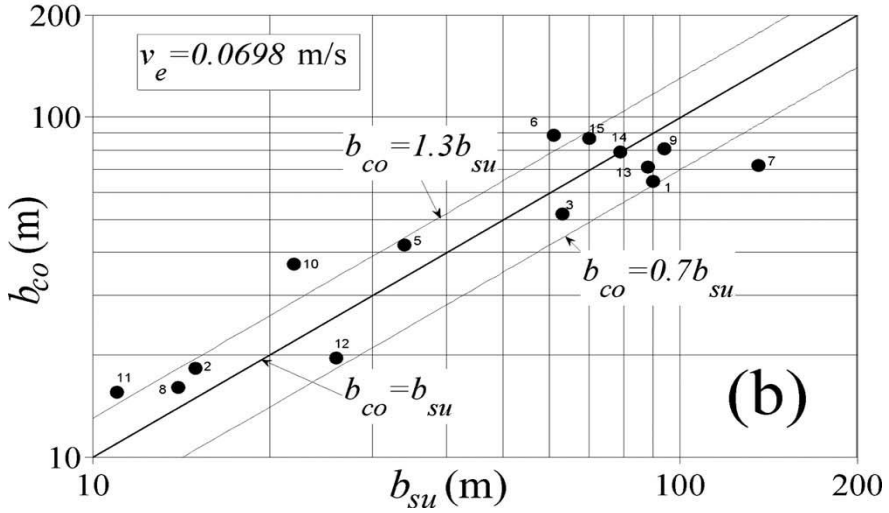

Figure 3. Predicted breach average width b_{co} versus observed one b_{su} for earthen dam failures which considered in the study of Macchione (2008) with applying v_e=0.0698 m/s

Table 1. Expressions for R, V, hc, dAb, dY, and l as Functions of Z and Y

Breach	$R =$	$V =$	$h_c =$	$\frac{dA_b}{dY}$	$l =$
Triangular	$\frac{1}{2}h_c \sin\beta$	$\left(\frac{1}{2}g\,h_c\right)^{\frac{1}{2}}$	$\frac{4}{5}(Z-Y)$	$-2(Z_M-Y)\tan\beta$	$(Z_M-Y)\,\frac{S_u+S_d}{2}+\,W_c$
Trapezoidal	$\frac{h_c(h_c-2Y)}{2(\frac{h_c}{\sin\beta}-Y)}$	$\left[g\frac{h_c-2Y}{2(h_c-Y)}h_c\right]^{\frac{1}{2}}$	$\frac{1}{5}\left[2Z+3Y+(9Y^2+4Z^2-8YZ)^{\frac{1}{2}}\right]$	$-2Z_M\tan\beta$	$Z_M\frac{S_u+S_d}{2}+\,W_c$

The temporal evolution of the variable Z is obtained by the continuity equation of volume W stored in the reservoir.

$$Q_i - \sum Q_{ow} - Q = \frac{dW}{dt} \tag{2.11}$$

in which Q_i = inflow rate to the reservoir, $\sum Q_{ow}$ = sum of outflow discharges through the outlet works; and Q= outflow discharge through the breach. To take the reservoir shape into consideration, the stored volume W is given as a function of Z by the level-reservoir volume curve, reported in what follows:

$$W = W_0 Z^{\alpha_0} \tag{2.12}$$

in which W_0 coefficient and α_0 actually varies between 1 and 4 (Marone, 1971). If Q_i and $\sum Q_{ow}$ = are negligible with respect to Q, the continuity equation can be expressed as:

$$\frac{dZ}{dt} = -Q\frac{Z^{1-\alpha_0}}{\alpha_0 W_0} \tag{2.13}$$

Moreover, the relation for discharge Q in the triangular breach and the trapezoidal breach is given by the following equations respectively:

$$Q = (\frac{1}{2}g)^{1/2}\left[\frac{4}{5}(Z-Y)\right]^{5/2}\tan\beta \tag{2.14}$$

$$Q = (\frac{1}{2}g)^{1/2}\left[h_c(\mathrm{h}_c - 2Y)\right]^{3/2}(\mathrm{h}_c - \mathrm{Y})^{-1/2}\tan\beta \tag{2.15}$$

By substituting Eqs. (2.14) and (2.15) into Eq. (2.13), one obtains:

$$\frac{dZ}{dt} = -(\frac{4}{5})^{5/2}(\frac{g}{2})^{1/2}\frac{Z^{1-\alpha_0}}{\alpha_0 W_0}(Z-Y)^{5/2}\tan\beta \qquad (2.16)$$

$$\frac{dZ}{dt} = -\frac{Z^{1-\alpha_0}}{\alpha_0 W_0}(\mathrm{h}_c - 2\,\mathrm{Y})\,\mathrm{h}_c\left[\frac{g(h_c-2Y)}{2(h_c-Y)}h_c\right]^{1/2}\tan\beta \qquad (Y\langle 0) \qquad (2.17)$$

Therefore, the generation of outflow hydrograph in the first part of the phenomena (triangular breach) is calculated by equations (2.5) and (2.16) and the consequence discharge Q is given by Eq. (2.14). When the breach section becomes trapezoidal, the breach hydrograph is calculated by equations (2.5) and (2.17) and Q is given by equation (2.15). The initial conditions are given by the initial water level *Z(0)* in the reservoir and initial breach bottom elevation *Y(0)*, at time $t = 0$.

Chapter 3

The power function for representing the reservoir rating curve: morphological meaning and suitability for dam breach modeling

3.1 Introduction

Numerical computations concerning reservoirs, and in particular those that specifically have to describe filling and emptying processes, including those in dam breaching calculations, require the availability of information on the volume stored in the reservoir as a function of water depth. Since the reservoirs have a natural topography, their geometry cannot be expressed exactly by an analytical formula. For this reason, usually detailed tables are utilized for this purpose, where each value of elevation from bottom to top has a corresponding value for lake surface and reservoir volume. These tables very often are plotted and are known as elevation - volume or elevation - area curves. However, in the

cases for which there is a scarcity of data, we have to interpolate the values of the table to achieve an analytical expression. Usually a polynomial function is the most appropriate one, but unfortunately it requires the assessment of several parameters and this may result in some difficulties in the systematic studies of flood control reservoirs or dam breach aimed at giving generalized solutions based on a number of characteristic parameters. In particular the systematic study of the dam breach problem is the reason which lead to this part of the research. As an example, if one wishes to develop the hydrograph computations using a non dimensional formulation, it is fundamental to decrease the number of parameters as much as possible. In this context the use of a polynomial function in the elevation-volume curve is not feasible. For this purpose, if applicable, it would be advantageous to express the reservoir rating curve, also called elevation-volume curve, using the power function, because this has the advantage of being a monomial function and only one parameter needs to be estimated. This expression has been already used in the past by other authors (Marone, 1971; Michels, 1977). Macchione (1986, 1989 & 2008), Macchione and Rino (2008) and De Lorenzo and Macchione (2011 & 2014) have used the power function in dam breach modelling for the calculation of flood hydrograph and peak discharge. However, some authors considered the use of this kind of expression an approximate approach (ASCE/EWRI, 2011). In this part of research, the high accuracy and suitability of this approach in representation of

the morphology of the reservoirs, at least for dam breach studies, have been shown. As a consequence, it will be shown that its use in numerical modelling does not affect the accuracy of calculations. This will be demonstrated in this part of thesis by analysing the suitability of the power function as an interpolating equation for reservoirs located in three different regions of the world, in order to verify the applicability of the function for various geological and geomorphological contexts. The results shown in the next sections can be found in (Macchione, et al., 2015).

3.2 Database used, investigation method and results

3.2.1 Database used

It is not easy to gather accurate surveys with a sufficient amount of data about the bathymetry of reservoirs from different regions of the world. Sometimes data are not open to the public and are not easily shared. However, on the Internet a very accurate database for many artificial reservoirs and dams from Texas is available at: *http://www.twdb.texas.gov/surfacewater/58surveys /completed/list/ index.asp*. Data available at this web site are the consequence of a survey campaign carried out by the Texas Water Development Board (TWDB) started in 1991 for monitoring rates of sediment deposition in the reservoirs. The campaign included more than 100 reservoirs defined as “major reservoirs”; by definition, a major reservoir has a conservation storage capacity of 5000 acre −

feet (6.2×10^6 m^3) or greater. Surveys have been replicated over the years, therefore more than one set of surveyed data may be available for some reservoirs. In order to have a bathymetry as close as possible to the early life of the reservoir, when more survey reports were available, the oldest has been considered for this study. The surveys were carried out with water level close to the top of conservation pool elevation, therefore for every dam, data are available up to this elevation. Technical details about criteria, tools and instruments used for the surveys can be found in the detailed reports available in the aforementioned web site. In these part of thesis, results of the surveys are shown in the tables "Reservoir volume table" or "Reservoir area table". Volumes and areas are given in function of the elevation; each step in elevation is one tenth of a foot. In this analysis, in order to avoid the inclusion of reservoirs in which an abnormal sediment deposition occurred over time, the ones experiencing a loss of available volume larger than 20% since first filling have been ignored. Moreover off-channel reservoirs, reservoirs whose reports did not have the tables, or with missing or corrupt values for crucial data like crest elevation, have been excluded. In conclusion, 65 reservoirs have been considered eligible for the analysis (Macchione, et al., 2015). Fig. 4 shows how the reservoirs here analysed are characterized by very variegated shapes.

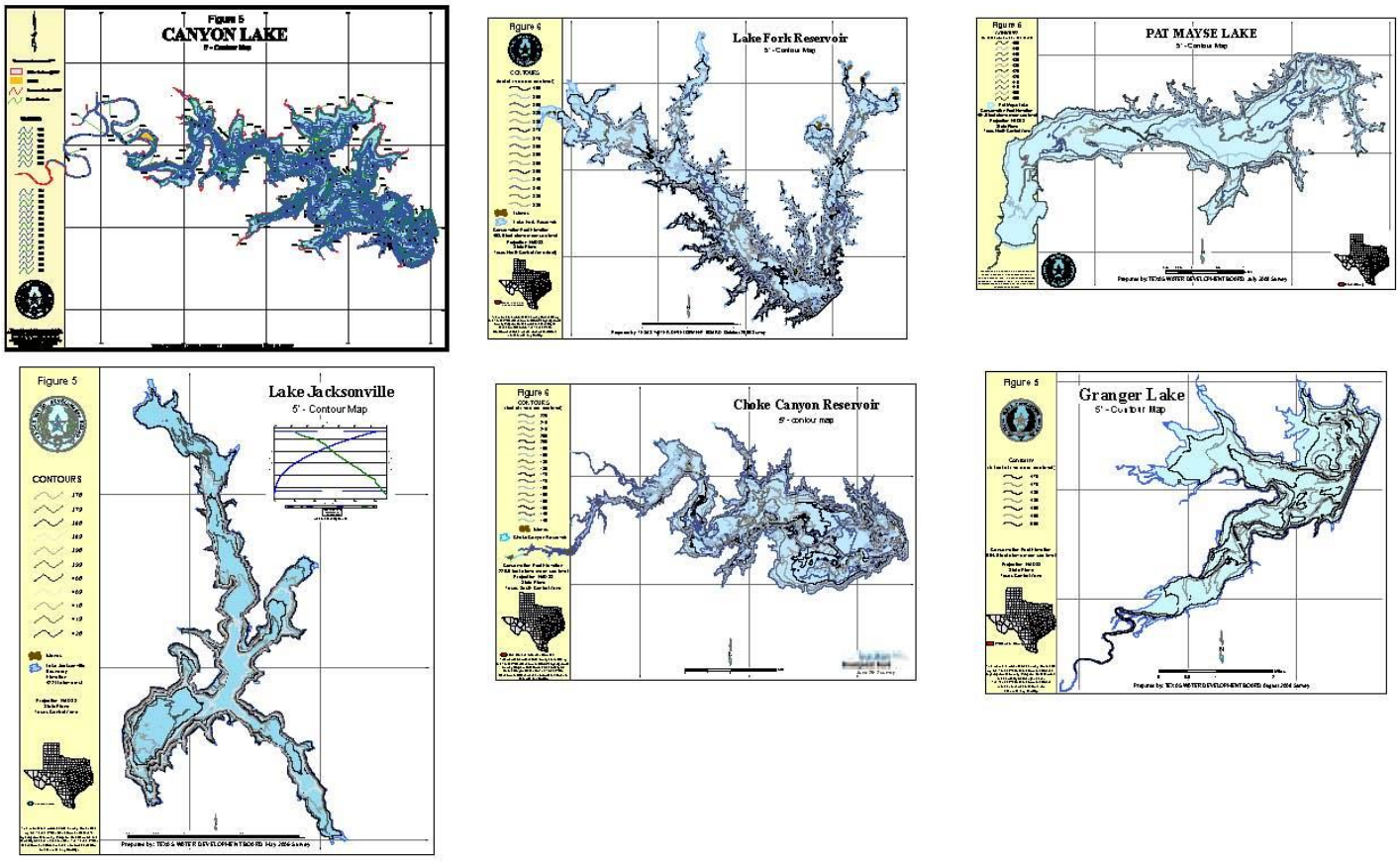

Figure 4. Some of the reservoirs from Texas considered in this study

This investigation also covers those technical situations for which high quality and very detailed tables, like the ones from TWDB, are not available. In particular, data about dams and reservoirs from Utah (USA), available at the web site of the Utah Division of Water Rights *http://www.waterrights.utah.gov/cgi-bin/damview.exe*, have been analysed. In this case, only reservoirs having enough data to cover all the aspects of the present analysis have been selected. Moreover, among these, only the ones having a hydraulic height greater than 10 m or having a stored volume greater than 10^6 m^3 have been considered. As will be clear by the plots, the number of available points for each reservoir of the Utah database is much smaller if compared to TWDB reservoirs, except for one case which has a large number of points (BOR Jordanelle dam). From Utah we were able to find 18 reservoirs for this study. Finally, we have analysed 14 reservoirs in Calabria (Italy), having stored volumes greater than 10^6 m^3 or a dam higher than 15 m. The interest in the study of reservoirs in these parts of the world lies in the fact that they belong to very different regions. Utah is a rocky region, but has almost three different geomorphological regions: the Rocky Mountains, the Great Basin, and the Colorado Plateau. Texas is a transition zone between the Great Plains and the Rocky Mountains; in this State plains, hills and plateau are the dominant landscape. Calabria is a narrow peninsula between the Tyrrhenian and the Ionian seas. Due to the morphological configuration of the land, the basins have a very limited extent and high slopes.

3.3 Verification of the suitability of the equation for the description of the reservoir morphology

Data used in this study have been interpolated using the following equation:

$$W = W_0 Z^{\alpha_0} \tag{3.1}$$

Values of the terms W_0 and α_0 have been obtained by the least squares method. Table 2 shows the results of the investigation.

Table 2. Reservoir considered in the analysis

Region	N. of cases	Av. α_0	SQM α_0	Min α_0	Max α_0	Av. R^2	SQM R^2	Min R^2	Max R^2
Texas	65	3.107	0.645	2.29	5.46	0.99942	0.000858	0.9941173	0.999983
Utah	18	2.71	0.588	1.75	3.917	0.998558	0.002668	0.989728	0.999996
Calabria	14	2.715	0.58	1.819	4.269	0.999457	0.000356	0.998503	0.999952

As expected, average values of α_0 have been found between 2 and 3. Moreover, higher values of α_0 hardly exceed 4. The results are remarkable, concerning the quality of interpolation. Average values of R^2 are close to 1 for each region. Therefore Eq. (3.1) is an excellent approximation for the elevation volume table. It can be also interesting to have a closer insight and check the adaptation of the power equation to the table as a function of the filling percentage in the reservoir. This analysis has been carried out for each region. The results are presented

through some graphs in which the error ϵ is plotted versus the ratio W_t/W_{max}, where W_t is the volume read from the table for a given elevation and W_{max} is the maximum volume stored in the reservoir (Fig. 5 to 7). The parameter ϵ is the difference between the volume W_c computed by Eq. (3.1) and the surveyed one W_t scaled to respect the maximum volume W_{max}:

$$\varepsilon = \frac{W_c - W_t}{W_{\max}} \tag{3.2}$$

multiplying ϵ by the ratio $W_{max}=W_t$ we obtain the local error that one gets by using the curve in place of the table. So, in the Figures 5 to 7, the local error can be obtained by dividing the abscissa by the value of the ordinate. Figures 5 to 7 show that the error is very small throughout all the ordinate axis. For reservoirs of Texas the values are almost always in the range ±2% and so it is also for Calabria and Utah, although the amount of data available for those regions is smaller than the cases of Texas.

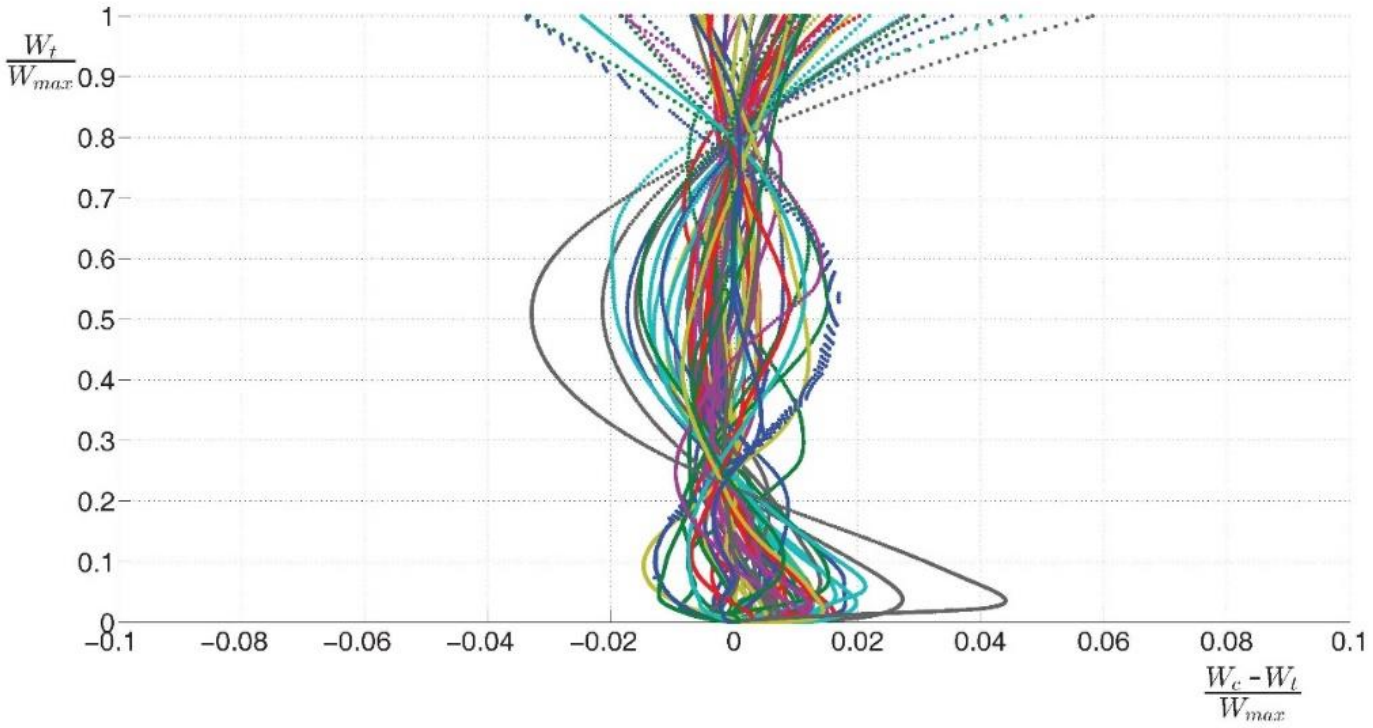

Figure 5. Texas: interpolation using all points available. Error versus percent of filling

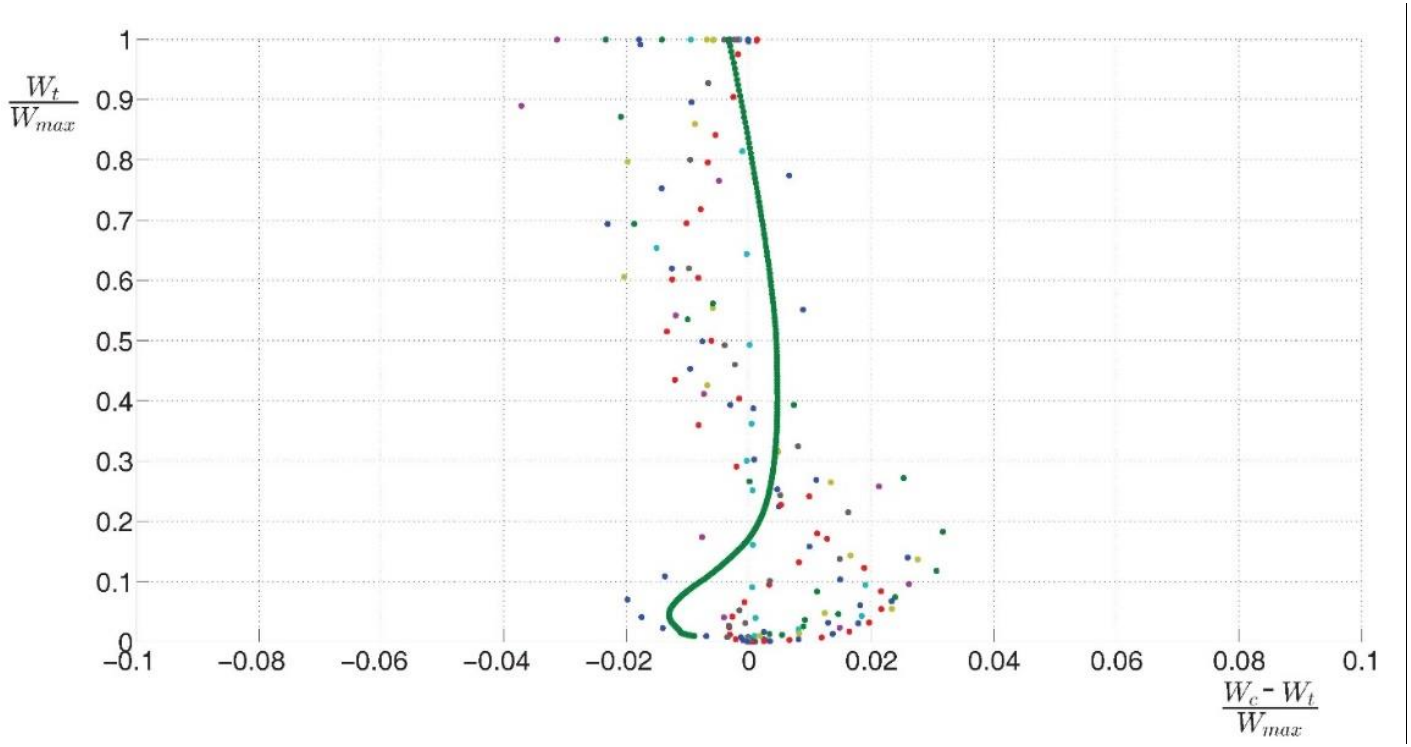

Figure 6. Utah: interpolation using all points available. Error versus percent of filling

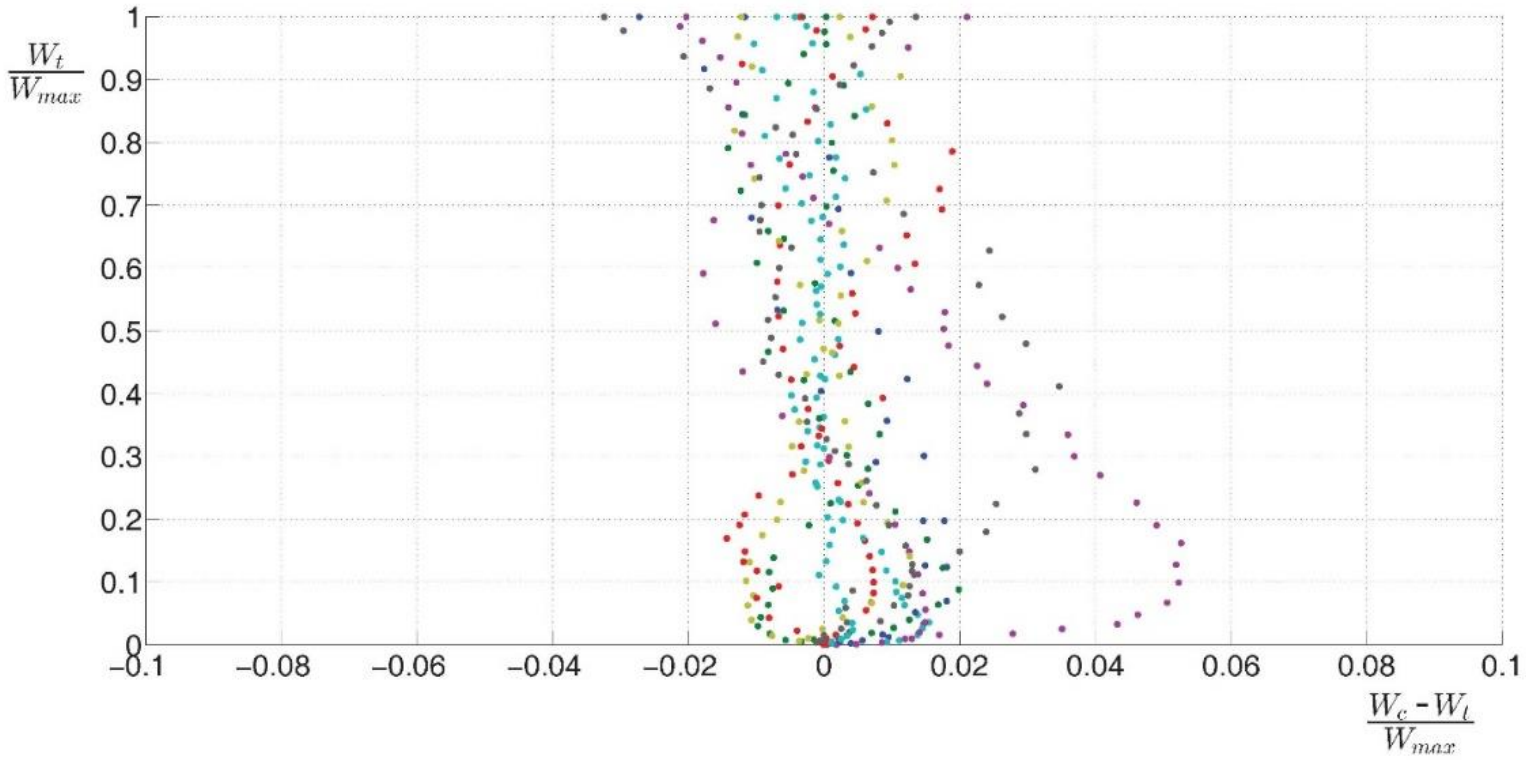

Figure 7. Calabria: interpolation using all points available. Error versus percent of filling

3.4 Determination of parameters for elevation-volume curve in limited data availability

Very often detailed data about reservoirs are missing or not readily accessible. Therefore, research studies or technical applications cannot rely on complete and reliable tables about elevations and the corresponding volumes, or lake area. In particular this situation is very common for dam breach studies concerning historical events. Very often lake area or stored volume are known only for few elevations, like conservation pool or maximum stored volume. It may be very interesting to know how accurate a volume-elevation curve obtained from a small number of points can be. If only two values of volume W_1 and W_2 are available with the corresponding elevations Z_1 and Z_2, the values of W_0 and α_0 can be obtained by the following equations:

$$\alpha_0 = \frac{\log W_1 - \log W_2}{\log Z_1 - \log Z_2} \tag{3.3}$$

$$W_0 = \frac{W_1}{Z_1^{\alpha_0}} \tag{3.4}$$

If both the surface S_r and the volume W_r are known at the corresponding generic elevation Z_r, the value of α_0 can be computed by (Macchione, 2008):

$$\alpha_0 = \frac{Z_r S_r}{W_r} \tag{3.5}$$

and W_0 is given by:

$$W_0 = \frac{W_r}{Z_r^{\alpha_0}} \tag{3.6}$$

It may be very interesting to compute the error produced by these two methods for the calculation of W_0 and α_0. For this purpose, we have considered two elevations and their relative volumes and areas. The upper point was chosen at the normal pool level (highest elevation available), and the other one was chosen at a lower elevation. A sensitivity analysis has been carried out (Fig. 8-13), and the errors that are committed using different elevations for the lower point have been analysed. In particular the elevation of the lowest points was set in order to have a volume equal to 20%, 30%, 40%, 50% of the normal pool volume. Obviously, the error is nil in correspondence of the two selected points and has the maximum value in a certain point comprised between the selected points. The more is the distance between the selected points, the higher is the maximum error. The same is for the maximum error in the region between 0 and the lowest point. But in all the cases, the greatest values of errors are very low. Figures 8 to 10 show the results obtained setting the lowest point at 40% of the normal pool volume. The curves, whose parameters are calculated by Eq. (3.5) and (3.6), worsen more rapidly as the volume decreases (Fig 11-13); however, even for this method, the greatest values of error are almost always in the range ±5%. In the next section the suitability of the curve will be analysed for the dam breach problem.

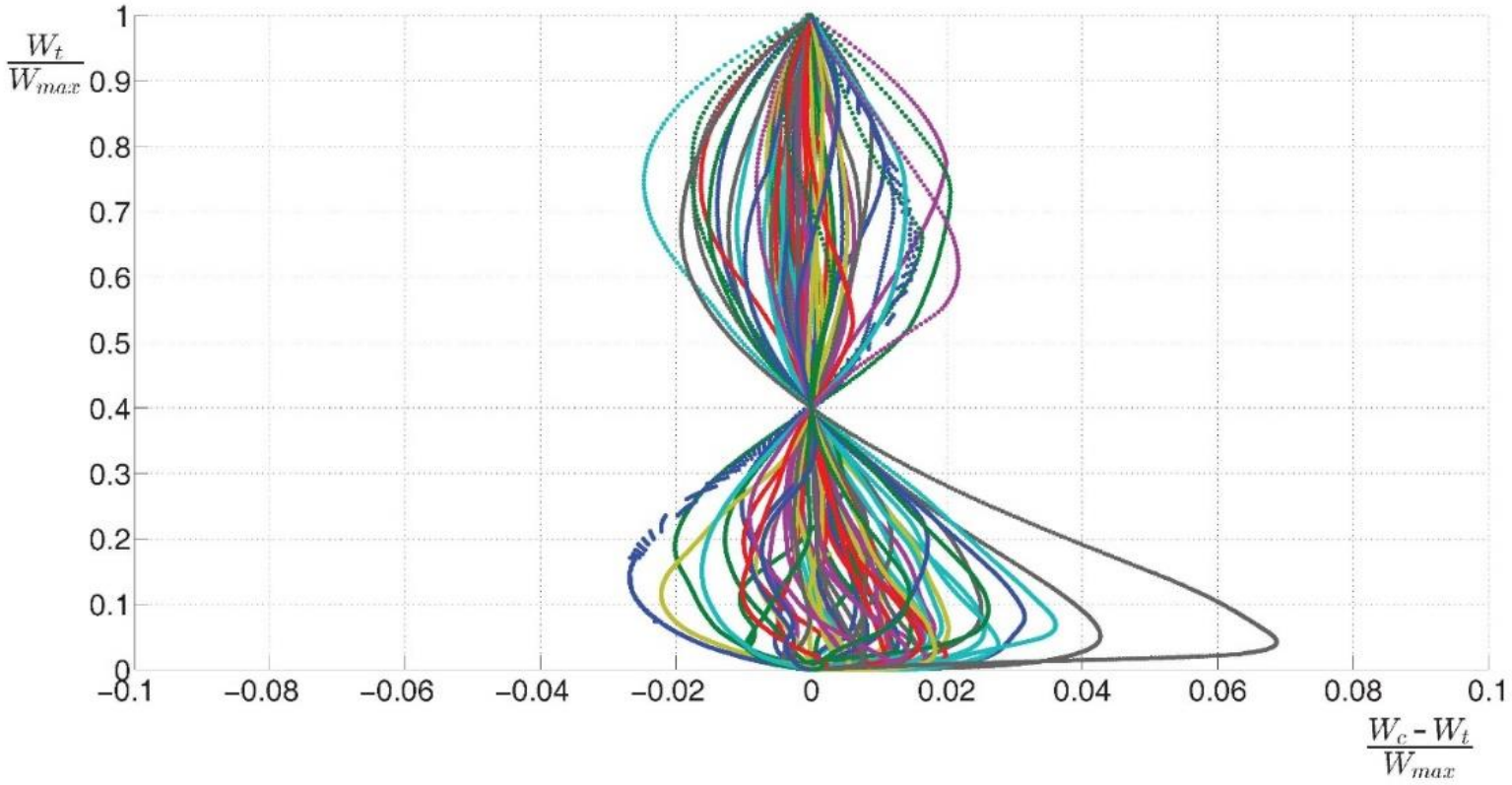

Figure 8. Error versus filling percentage of reservoirs from Texas database: interpolation based on two points only (the lowest one is located at 40% of normal pool level volume)

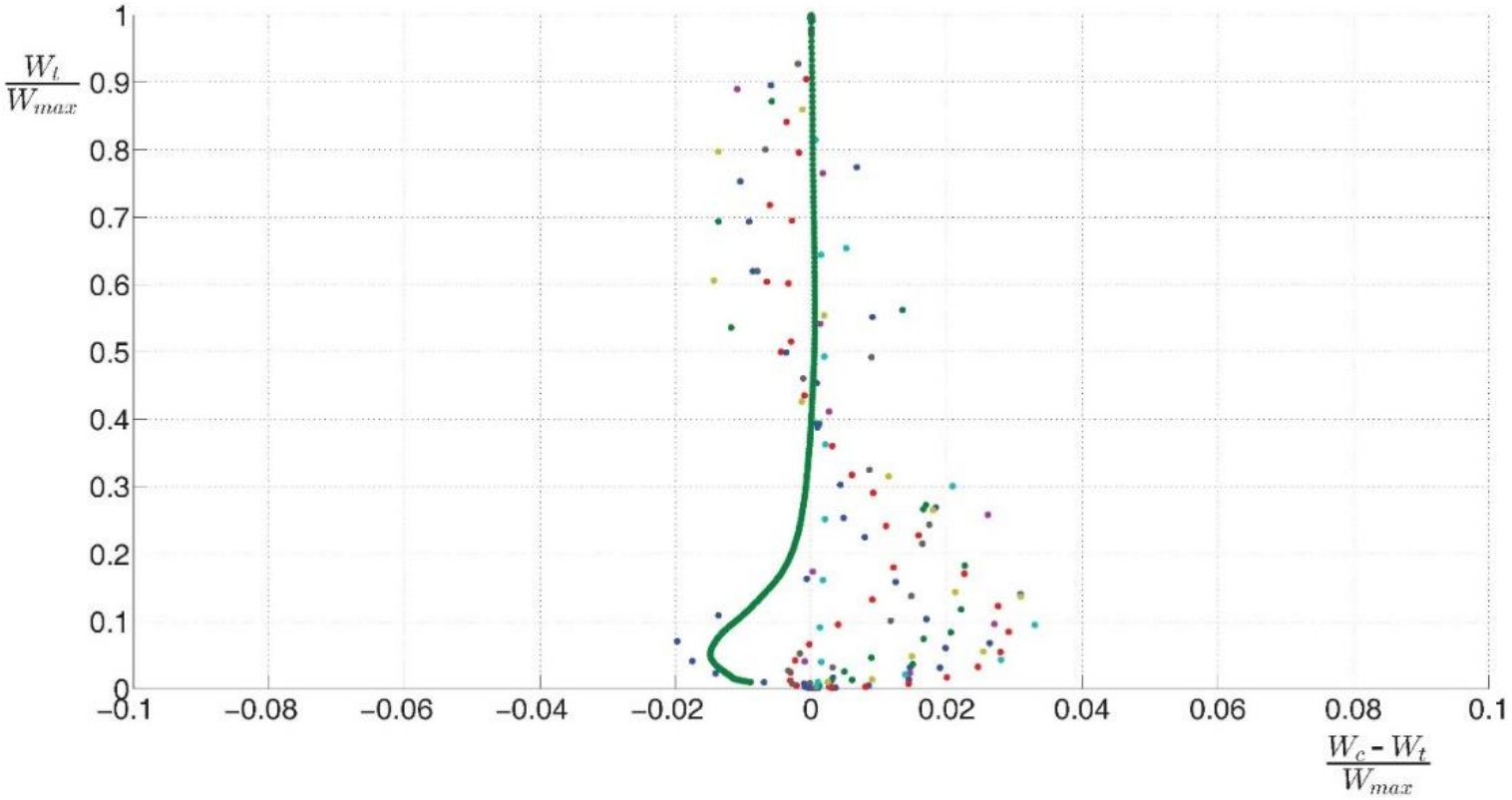

Figure 9. Error versus filling percentage of reservoirs from Utah database: interpolation based on two points only (the lowest one is located at 40% of normal pool level volume)

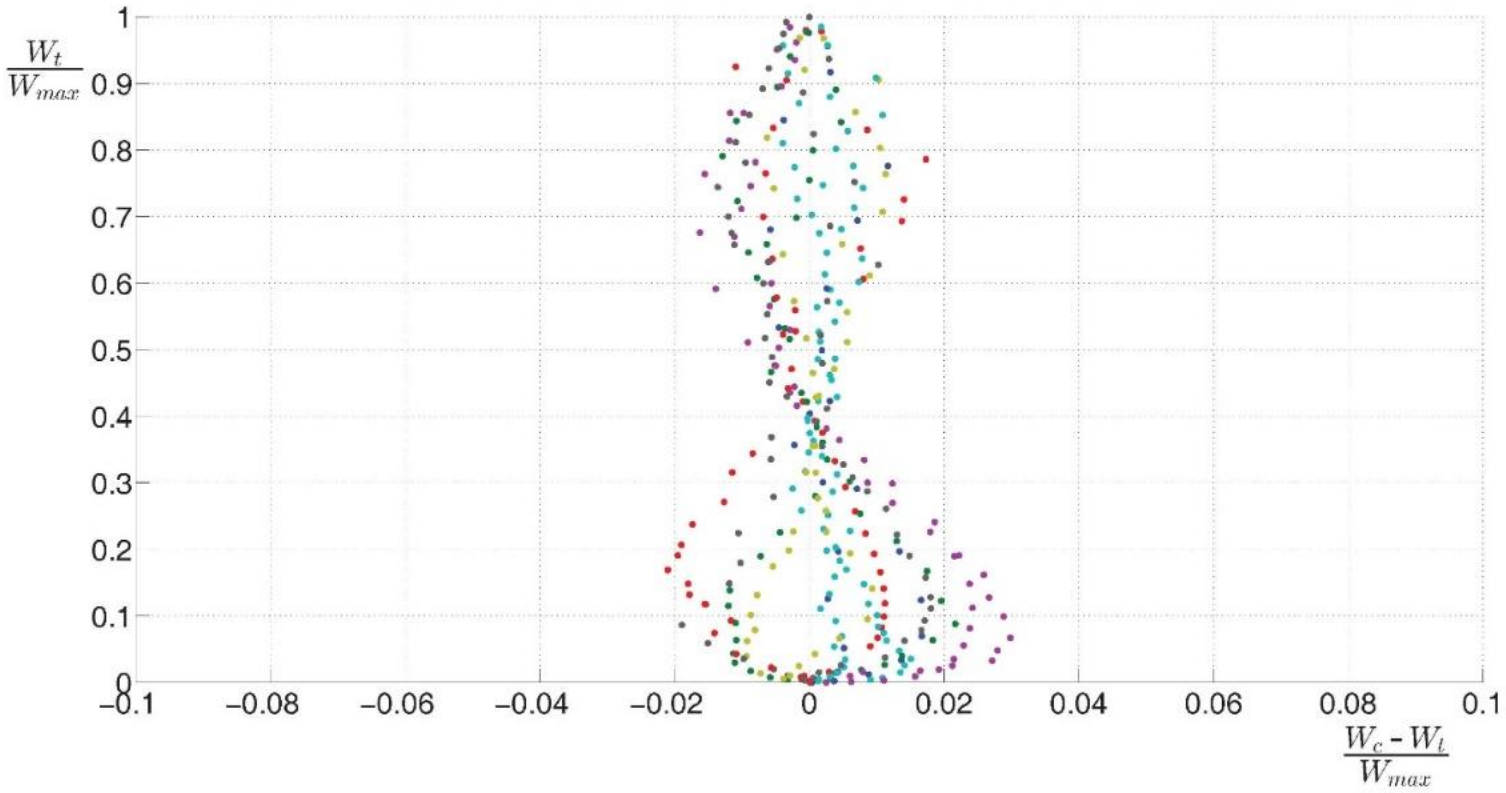

Figure 10. Error versus filling percentage of reservoirs from Calabria database: interpolation based on two points only (the lowest one is located at 40% of normal pool level volume)

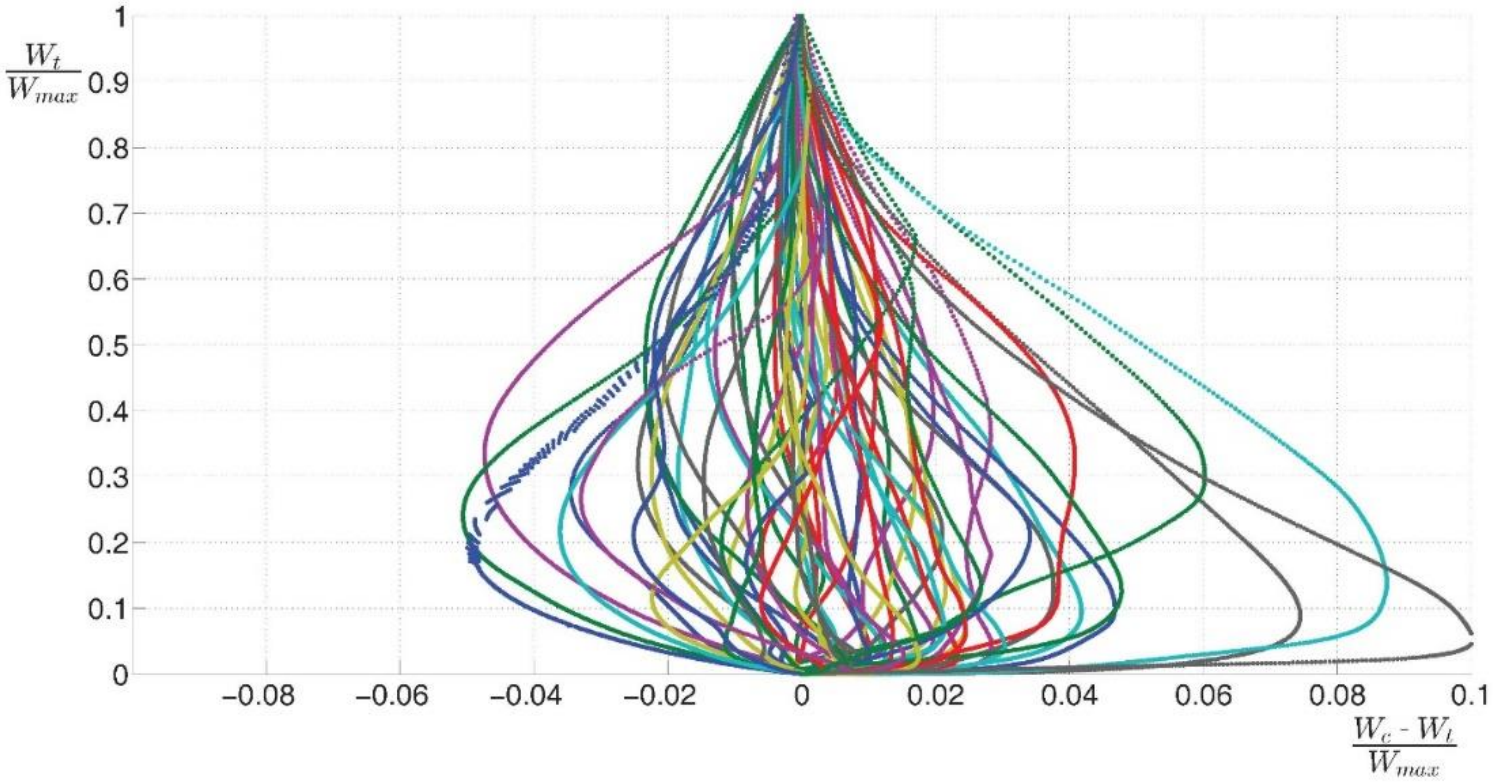

Figure 11. Error versus filling percentage of reservoirs from Texas database: interpolation based on two points only (the lowest one is located at 30% of normal pool level volume)

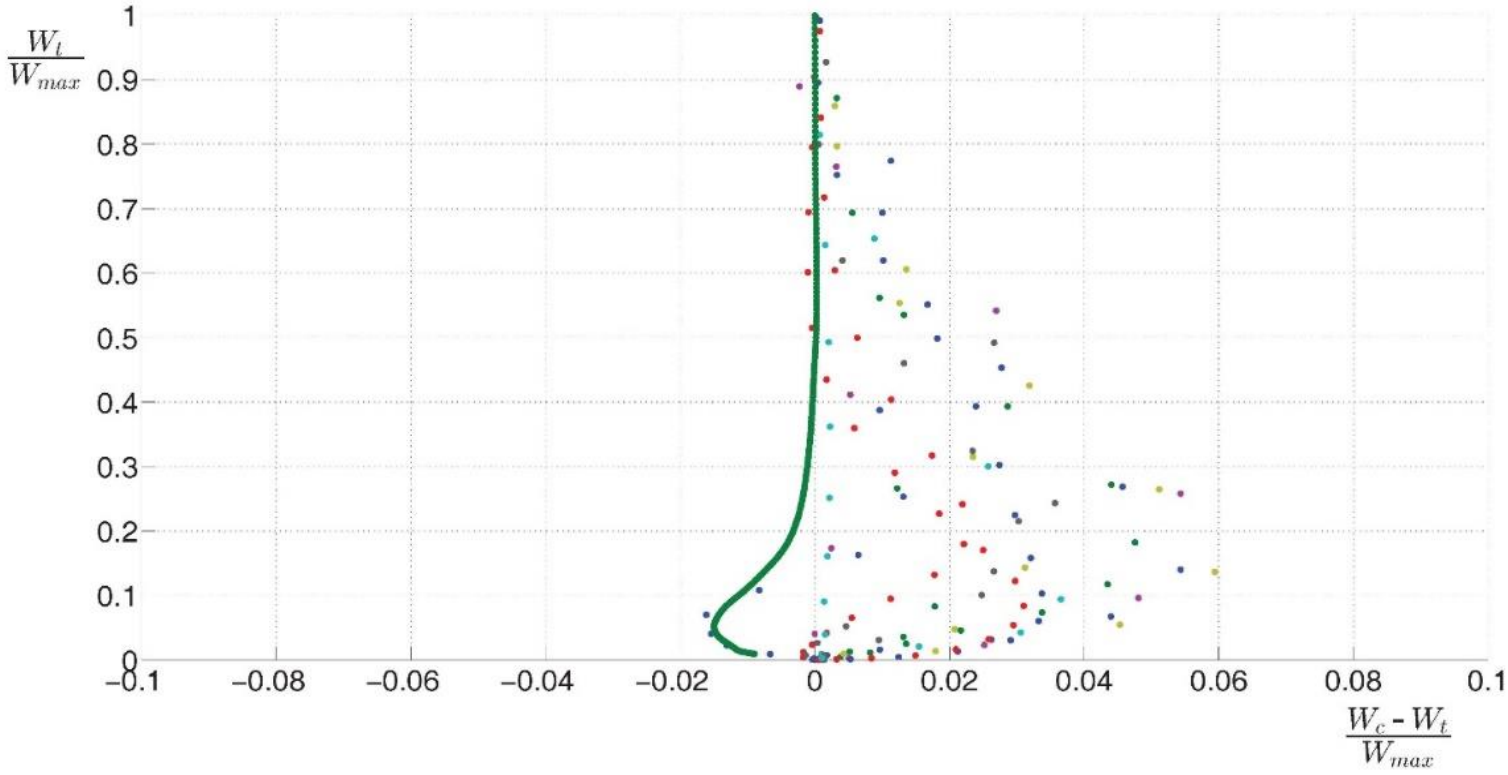

Figure 12. Error versus filling percentage of reservoirs from Utah database: interpolation based on two points only (the lowest one is located at 30% of normal pool level volume)

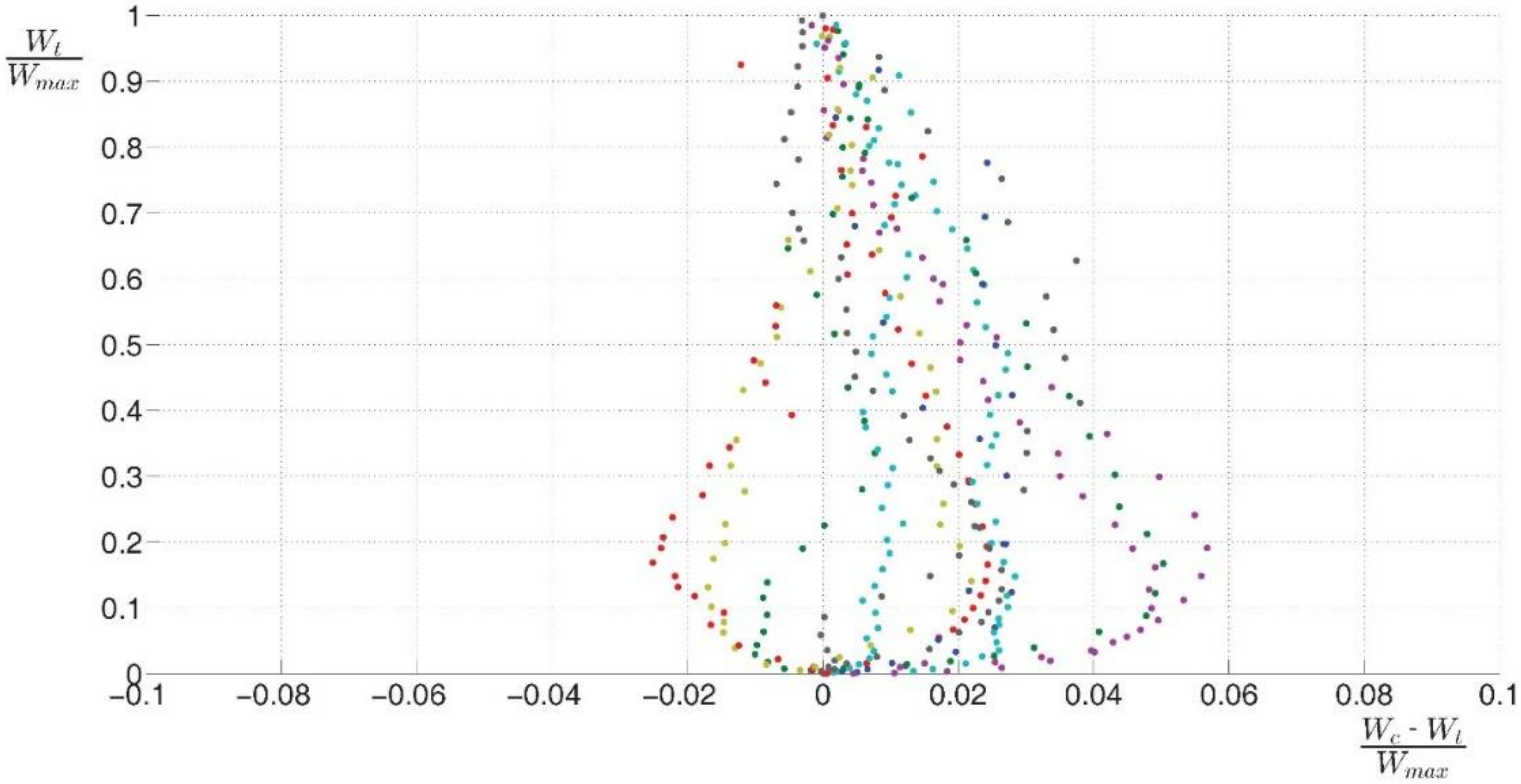

Figure 13. Error versus filling percentage of reservoirs from Calabria database: interpolation based on two points only (the lowest one is located at 30% of normal pool level volume)

3.5 Influence of the use of equation Eq. (3.1) on the outflow hydrograph due to dam breach events

In order to assess the influence of the use of Eq. (3.1) on the outflow hydrograph due to the breaching of dams, a subset of only earthfill dams has been extracted from the reservoirs already studied in the previous sections. In particular, 50 earthfill dams have been extracted from the Texas database, 16 dams from the Utah database, and 6 dams from the Calabria database. For each dam the outflow hydrograph has been calculated using the model proposed by Macchione (2008). The same case studies have been simulated introducing a slight modification to the model that allows the direct use of the surface-elevation table. In particular *S(h)* has been used in place of *W*(*h*) as in the mass conservation equation of the model we find the derivative *dW/dZ* and not actually the volume, and as said in the previous sections *dW/dZ* is the lake area at elevation *Z*. In order to assess the suitability of Eq. (3.1) in the approximation of the volume-elevation table on the outflow hydrograph, the differences between the values of some variables computed using the methods shown in the previous section have been calculated. In particular the peak discharges Q_p, *W*, the time to peak discharge T_p and the final average breach width B_m have been compared. Tables 3 to 8 show average values, maximum values and standard deviations. Moreover the average value of parameter R^2 reported in those tables, show the level of accuracy provided by the analysed interpolation methods.

Table 3. Method of interpolation: least square of all elevation-volume data

Region	N. Cases	Avg. R^2	SD R^2	Max. R^2	Min R^2	Avg. $\frac{\Delta Q_p}{Q_p}$%	SD $\frac{\Delta Q_p}{Q_p}$%	Avg. $\frac{\Delta W}{W}$%	SD $\frac{\Delta W}{W}$%	Avg. $\frac{\Delta T_p}{T_p}$%	SD $\frac{\Delta T_p}{T_p}$%	Avg. $\frac{\Delta B_m}{B_m}$%	SD $\frac{\Delta B_m}{B_m}$%
Texas	15	0.999567	0.000537	0.999983	0.996985	1.062	1.910	0.684	1.262	0.438	0.739	0.333	0.647
Utah	16	0.999996	0.000701	0.997594	0.999416	0.235	1.140	-0.764	1.239	-1.562	3.122	-0.889	1.462
Calabria	6	0.999494	0.000438	0.999722	0.998603	0.799	2.143	0.292	1.328	-0.403	0.844	0.110	0.745
Wgt. Avg		0.999656				0.856		0.33		-0.076		0.0429	

Table 4. Method of interpolation: Eq. (3.5) and Eq. (3.6)

Region	N. Cases	Avg. R^2	SD R^2	Max. R^2	Min R^2	Avg. $\frac{\Delta Q_p}{Q_p}$%	SD $\frac{\Delta Q_p}{Q_p}$%	Avg. $\frac{\Delta W}{W}$%	SD $\frac{\Delta W}{W}$%	Avg. $\frac{\Delta T_p}{T_p}$%	SD $\frac{\Delta T_p}{T_p}$%	Avg. $\frac{\Delta B_m}{B_m}$%	SD $\frac{\Delta B_m}{B_m}$%
Texas	50	0.997193	0.99409	0.999941	0.97793	0.026	1.543	0.002	0.425	-0.257	2.004	-0.116	0.49
Utah	16	0.995797	0.003484	0.999965	0.990391	-1.037	1.012	-0.048	0.681	-3.258	3.148	-1.384	1.521
Calabria	6	0.995944	0.003776	0.999637	0.989154	-1.033	0.752	0.141	0.445	-1.403	1.400	-0.306	0.536
Wgt. Avg		0.996778				-0.298		0.002		-1.019		-0.414	

Table 5. Method of interpolation: two points, the lower at 20%

Region	N. Cases	Avg. R^2	SD R^2	Max. R^2	Min R^2	Avg. $\frac{\Delta Q_p}{Q_p}$%	SD $\frac{\Delta Q_p}{Q_p}$%	Avg. $\frac{\Delta W}{W}$%	SD $\frac{\Delta W}{W}$%	Avg. $\frac{\Delta T_p}{T_p}$%	SD $\frac{\Delta T_p}{T_p}$%	Avg. $\frac{\Delta B_m}{B_m}$%	SD $\frac{\Delta B_m}{B_m}$%
Texas	50	0.999204	0.000976	0.999974	0.99516	0.578	1.307	0.014	0.402	0.041	0.867	-0.014	0.196
Utah	16	0.998673	0.000999	0.999948	0.996522	1.365	1.587	0.046	0.623	0.304	2.290	-0.332	0.986
Calabria	6	0.999001	0.000876	0.999602	0.997306	1.091	2.113	0.146	0.448	-0.212	0.451	0.127	0.221
Wgt. Avg		0.999069				0.796		0.032		0.078		-0.073	

Table 6. Method of interpolation: two points, the lower at 30%

Region	N. Cases	Avg. R^2	SD R^2	Max. R^2	Min R^2	Avg. $\frac{\Delta Q_p}{Q_p}$%	SD $\frac{\Delta Q_p}{Q_p}$%	Avg. $\frac{\Delta W}{W}$%	SD $\frac{\Delta W}{W}$%	Avg. $\frac{\Delta T_p}{T_p}$%	SD $\frac{\Delta T_p}{T_p}$%	Avg. $\frac{\Delta B_m}{B_m}$%	SD $\frac{\Delta B_m}{B_m}$%
Texas	50	0.999312	0.000835	0.999972	0.995399	0.324	0.893	0.007	0.412	-0.105	0.898	-0.064	0.234
Utah	16	0.998916	0.00628	0.999957	0.997626	0.970	1.172	0.029	0.631	-0.297	1.899	-0.515	0.954
Calabria	6	0.999189	0.000551	0.999562	0.998109	0.791	1.403	0.146	0.448	-0.402	0.188	0.068	0.192
Wgt. Avg		0.999214				0.506		0.023		-0.172		-0.153	

Table 7. Method of interpolation: two points, the lower at 40%

Region	N. Cases	Avg. R^2	SD R^2	Max. R^2	Min R^2	Avg. $\frac{\Delta Q_p}{Q_p}$%	SD $\frac{\Delta Q_p}{Q_p}$%	Avg. $\frac{\Delta W}{W}$%	SD $\frac{\Delta W}{W}$%	Avg. $\frac{\Delta T_p}{T_p}$%	SD $\frac{\Delta T_p}{T_p}$%	Avg. $\frac{\Delta B_m}{B_m}$%	SD $\frac{\Delta B_m}{B_m}$%
Texas	50	0.999207	0.001036	0.999981	0.994253	0.175	0.529	0.002	0.421	-0.189	1.041	-0.094	0.291
Utah	16	0.998213	0.001817	0.999973	0.99279	0.280	0.877	0.010	0.637	-1.306	2.030	-0.787	1.068
Calabria	6	0.999109	0.000684	0.999527	0.997815	0.407	1.029	0.145	0.448	-0.589	0.413	-0.007	0.259
Wgt. Avg		0.998978				0.218		0.016		-0.471		-0.241	

Table 8. Method of interpolation: two points, the lower at 50%

Region	N. Cases	Avg. R^2	SD R^2	Max. R^2	Min R^2	Avg. $\frac{\Delta Q_p}{Q_p}$%	SD $\frac{\Delta Q_p}{Q_p}$%	Avg. $\frac{\Delta W}{W}$%	SD $\frac{\Delta W}{W}$%	Avg. $\frac{\Delta T_p}{T_p}$%	SD $\frac{\Delta T_p}{T_p}$%	Avg. $\frac{\Delta B_m}{B_m}$%	SD $\frac{\Delta B_m}{B_m}$%
Texas	50	0.998964	0.001433	0.999979	0.992461	0.076	0.386	-0.001	0.428	-0.242	1.243	-0.113	0.347
Utah	16	0.99768	0.002656	0.999996	0.988789	-0.060	0.803	-0.007	0.648	-1.798	2.152	-0.928	1.098
Calabria	6	0.998813	0.001106	0.999626	0.996806	0.169	0.846	0.145	0.448	-0.721	0.710	-0.051	0.362
Wgt. Avg		0.998667				0.054		0.01		-0.628		-0.289	

The method which gave the best result, according to R^2, is of course the one using all the points available. For this reason, interpolations using all the points has the highest value of R^2. This method is directly followed by the one using two points, with the lowest one taken at W/W_m = 0.3 (which means 30% of normal pool volume). Then, in descending order of quality we found W/W_m = 0.20, 0.40, 0.50. The lowest quality was obtained with the parameters calculated by Eq. (5.3) and Eq. (6.3), although, even with this method, R^2 is still very close to 1 (R^2 = 0.9968). Anyway, the results of the model are not really much influenced by the method used for interpolation. Table 9 shows the results for the most representative variables. It is easy to realize that the variations are very small, and they almost never exceed 1%. In particular, the method giving the smallest errors in term of Q_p and W is that of Eq. (3.5) and Eq. (3.6), directly followed by the one using a line passing for two points, with the lowest at 50% of normal pool volume (W/W_m = 0.5). This evidence is easily explained, since the peak discharge usually occurs when the reservoir is still almost full and these two methods reduce the errors for the upper part of the volume-elevation table. However, the errors are always very small, so it is not necessary to say which one is better and to give a ranking of the most suitable methods. All the variants used for the calculation of the parameters of power law gave very good results for the calculation of dam breach hydrograph and breach parameters.

Table 9. Average errors on dam breach results using differents methods to estimate parameter of Eq. (3.1)

Interpolation	0.999656	0.856	0.330	-0.076	0.0429
Two points 20%	0.999069	0.796	0.032	0.078	-0.073
Two points 30%	0.999214	0.506	0.023	-0.172	-0.153
Two points 40%	0.998978	0.218	0.016	-0.471	-0.241
Two points 50%	0.998667	0.054	0.010	-0.628	-0.289
Derivative Eqs. 5 and 6	0.996778	0.002	0.002	-1.019	-0.414

3.5.1 Morphological meaning of exponent α_0

It is interesting to highlight that the exponent α_0 of the proposed equation has also a precise morphological meaning. In particular, if in Eq. (3.5) we put the values of the surface S_m and the volume W_m corresponding to the value of the maximum elevation Z_m, Eq. (3.5) represents the ratio between the volume that the reservoir would have if it were a cylinder with a base equal to S_m and height equal to Z_m and the actual volume of the reservoir. Therefore the exponent α_0 represents the degree of flaring of reservoir sides. In particular, $\alpha_0 = 1$ represents a reservoir with vertical sides. The more flared the reservoir is, the higher the value of α_0. In this study the maximum value of α_0 was 5.46 and the minimum value was 1.75. The average value of α_0 for all these regions is about 3(2.98).

3.5.2 Disappearance of the parameter W_0

Given the small errors in dam breach applications, the calculation of the parameters of volume-elevation curve can be carried out using only two points. In particular the first point should be the one corresponding to the initial volume of the reservoir. Using this approach, Eq. (3.1) can be rewritten as follows Macchione and Sirangelo (1990):

$$W = W_m \left(\frac{Z}{Z_m}\right)^{\alpha_0} \tag{7.3}$$

In this way, parameter W_0 "disappears" from Eq. (3.1) and it is replaced by the quantity $W_m / Z_m^{\alpha_0}$. This form of Eq. (3.1) strictly provides the initial volume W_m at the elevation $Z = Z_m$. So, it makes the error on the total volume stored initially in the reservoir equal to zero.

Chapter 4

Dam breach modelling: influence on downstream water levels and a proposal of a physically based module for flood propagation software

4.1 Introduction

Literature study has shown that there is a lack of papers about the influence exerted by methods used for computing the dam breach hydrograph on the flood hazard and, in particular, on the simulated maximum water levels. This topic seems to be very important and should be considered precisely for selecting a specific computing module to be nested in commercial propagation softwares. This module should be balance the need for a reasonable physical description of the phenomenon and, at the same time, limit as much as possible the maximum number of parameters which should be estimate to run the model. In particular,

this last issue gained importance in the context of the reduction of the entire modelling uncertainty, ranging from the generation to the propagation of flood events. For this reason, any time it is possible to have well-documented test cases, these are extremely useful for model validation. One of the few cases in this context is represented by the Big Bay dam, located in Lamar County, Mississippi (USA), which experienced a failure on 12 March 2004. This event has been studied by Yochum et al. (2008) and Altinakar et al. (2010) for a general reconstruction of the event. Following the work by Yochum et al. (2008), the main purpose of this part of thesis is the analysis of simplified models for dam breach simulation, in order to identify a method that, on the basis of the results obtained in terms of simulated maximum water levels downstream, might effectively represent a preferential approach for its implementation not only in the most common propagation software but also for its integration in flood information systems and decision support systems (Demir & Krajewksi, 2013; Qi & Altinakar, 2011). For the reasons explained above, attention here focuses on the parametric models, widely used for technical studies, and on the Macchione (2008) model, whose predictive ability and ease of use have been already mentioned. The analysis was carried out using both 1-D and 2-D flood propagation modelling. For the 1-D modelling, the reference solution is that proposed by Yochum et al. (2008) whose details will be highlighted in the following sections. In particular, the unsteady flow option implemented in the

HEC RAS software was used. For the 2-D analysis, the numerical model proposed by Costabile and Macchione (2015), based on the fully dynamic shallow water equations, was applied for the analysis of the effects on water levels downstream. The results shown in the next sections can be found in Macchione, et al. (2015 a & b).

4.2 Information related to Big Bay dam failure

The Big Bay dam breach happened in 2004, 12 years after its construction. The dam was composed of homogeneous material. It was 576 m long and 15.6 m high (excluding the foundations). Other relevant data are: Longitude/Latitude: 89°34'19.2" W; 31°10'57" N; maximum storage: 26,365,674 m^3; normal storage: 13,876,670 m^3; surface area: 3,642,171 m^2. For further information, the reader can refer to Yochum et al. (2008) and Altinakar et al. (2010). In NWS (2006) the following news was reported. "Beneath the dam is Bay Creek which flows into Lower Little Creek about 1 mile south of the dam. Lower Little Creek flows west into Marion county and then into the Pearl River 10 miles south of Columbia. At this time, a total of 104 homes or businesses have been damaged by the flood waters. Of the 104 damaged structures, 48 were completely destroyed, 37 sustained major damage and 19 sustained minor damage. In addition, 30 roads were damaged or closed during the event. The affected area stretched some 17 miles west of the dam to where Lower Little Creek meets the

Pearl River". A little while after the failure, the U.S. Geological Survey (USGS), in cooperation with the Natural Resources Conservation Service (NRCS) - U.S. Departments of Agriculture (USDA), measured 42 high water marks (HWM) throughout the flooded areas. The HWM positions are listed in Altinakar et al. (2010). The dam failure was induced by a piping phenomenon. The breach evolution is described in the event report by Burge (2004). According to the report, the embankment failed with the reservoir level at about 0.15-0.20 m above the normal pool elevation (84.73 m). During the event, Burge recorded the breach enlargement process providing the following estimations: uncontrolled release of the lake pool began at approximately 12:25 p.m.; 12:40 p.m. breach width along crest of dam is about 75 feet in width; 12:50 p.m. breach widened to about 150 feet; 1:10 p.m. breach widens to ±200 feet; 1:40 p.m. breach about 350 feet wide. Moreover, Burge reports that "at 2:25 p.m. flow continuing to slow, flood pool dropping rapidly, scour hole becoming visible" and "at 2:40 p.m. water surface at about 240 elevation, flow very stable". For this reason, it seems that the most significant part of the flow hydrograph was developed between the 12:25 until 2:40 p.m., so that the duration is 2 hr and 15 min. The final breach geometry, estimated by Yochum et al. (2008) considering the summer 2004 aerial photography, highlighted a bottom width equal to 70 m and the top width equal to 96.0 m. Therefore, the side slope (horizontal/vertical)

was 0.61 on the right side and 1.3 on the left one. The breach finally reached the original ground elevation (71.3 m).

4.3 Computation of dam breach hydrograph

4.3.1 The Macchione model (2008)

In this work, the Macchione (2008) has been used for the numerical simulation of the dam breaching hydrograph. The governing equations of the model can be found in Macchione (2008) and Macchione and Rino (2008). The range 0.05–0.10 m/s can be used for the calibration parameter v_e. In particular, the mean value 0.07 m/s should be used when cases of dams similar to those examined in Macchione (2008) have to be simulated. The numerical simulation of the event has been carried out using the available observed data concerning, essentially, the observed breach, total volume which came out from the breach and the reservoir emptying time. This observation has been described in the previous section and is reported in table 10.

Table 10. Observed data: breach information, discharge volume, reservoir emptying time

Breach data from Burge (2004)	Time	12:25	12:40	12:50	1:10 PM	1:40 PM
	Breach width	Breach initial formation	75 m	150 m	200 m	350 m
Summer 2004 aerial photography	Breach bottom width	70 m				
	Top width	96 m				
	Average width	83 m				
	Side slopes (Horizontal / Vertical)	0.61 (right hand) and 1.3 (left hand)				
Hydrograph	Volume	17,500,000 m^3				
	Duration	2.25 hours				

As noted by Macchione (2008), the representative parameter of the total eroded volume is the mean breach width and not the top one. For this reason, information about the temporal enlargement of top width is not so important because the temporal evolution of the breach shape is unknown. Therefore, the attention here is devoted to the final mean width of the breach reported by Yochum et al. (2008). Using the data related to the observed breach, three discharge hydrographs have been obtained using the Macchione (2008) model. Since the dam failure was induced by erosion at the base of the embankment, an initial triangular breach with height equal to dam height has been assumed for all the simulations. The first hydrograph (hereafter named M1) has been obtained using the Macchione (2008) model in predictive mode. This means that it assumed v_e =0.07 m/s and the side slope tan β=0.2 as suggested by Macchione (2008). The temporal evolution of the mean breach width ($b_{average}$) is shown in figure 14. The second hydrograph (hereafter called M2) (see figure 15) has been computed assuming v_e=0.07 m/s and, as valued for slide slope, tanβ=0.955 that is the mean value observed for the aerial picture. The third hydrograph (hereafter named M3) has been obtained imposing tan β=0.2 and assuming v_e =0.09 m/s that is that value for which the simulated mean value of the final breach is equal to that estimated from the aerial picture. The results are shown in figure 16.

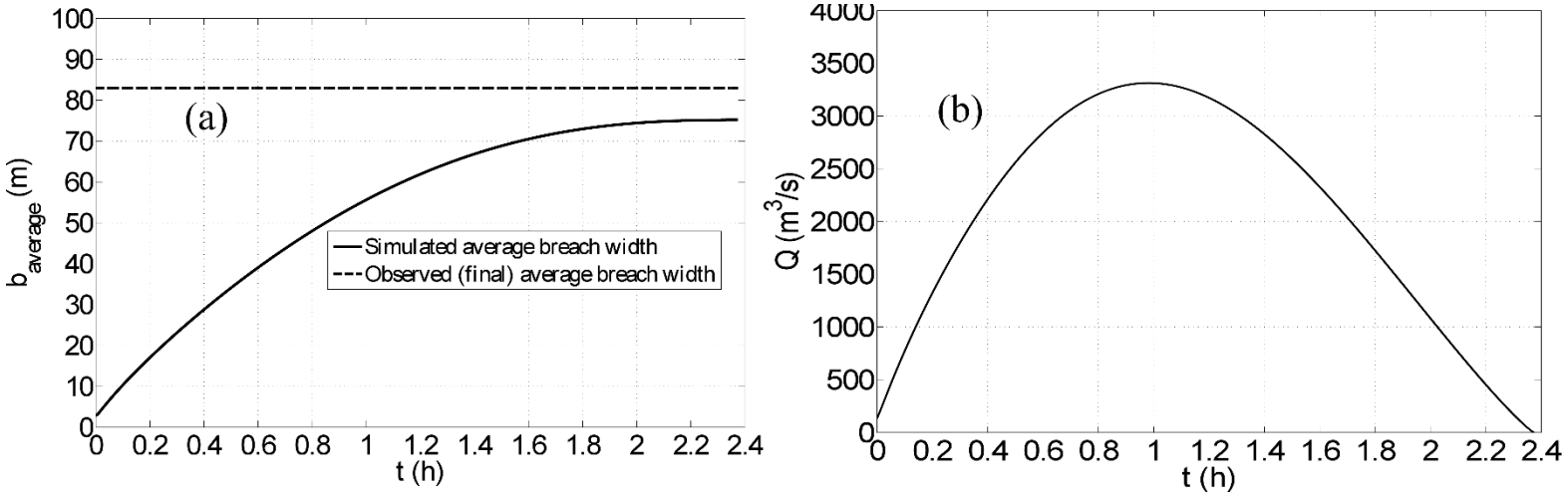

Figure 14. Simulation of the temporal behavior of both the mean breach width and the hydrograph using the Macchione (2008) model: v_e=0.07 m/s e tanβ=0.2 (M1 hydrograph)

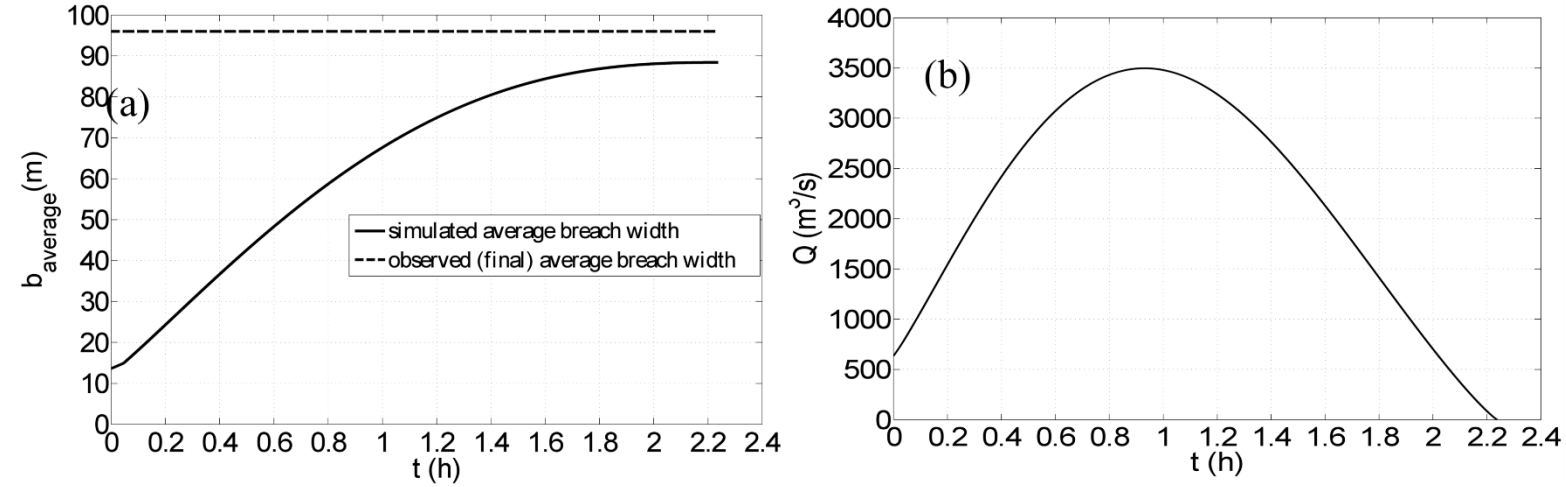

Figure 15. Simulation of the temporal behavior of both the mean breach width and the hydrograph using the Macchione (2008) model: v_e =0.07 m/s e tanβ=0.955 (M2 hydrograph)

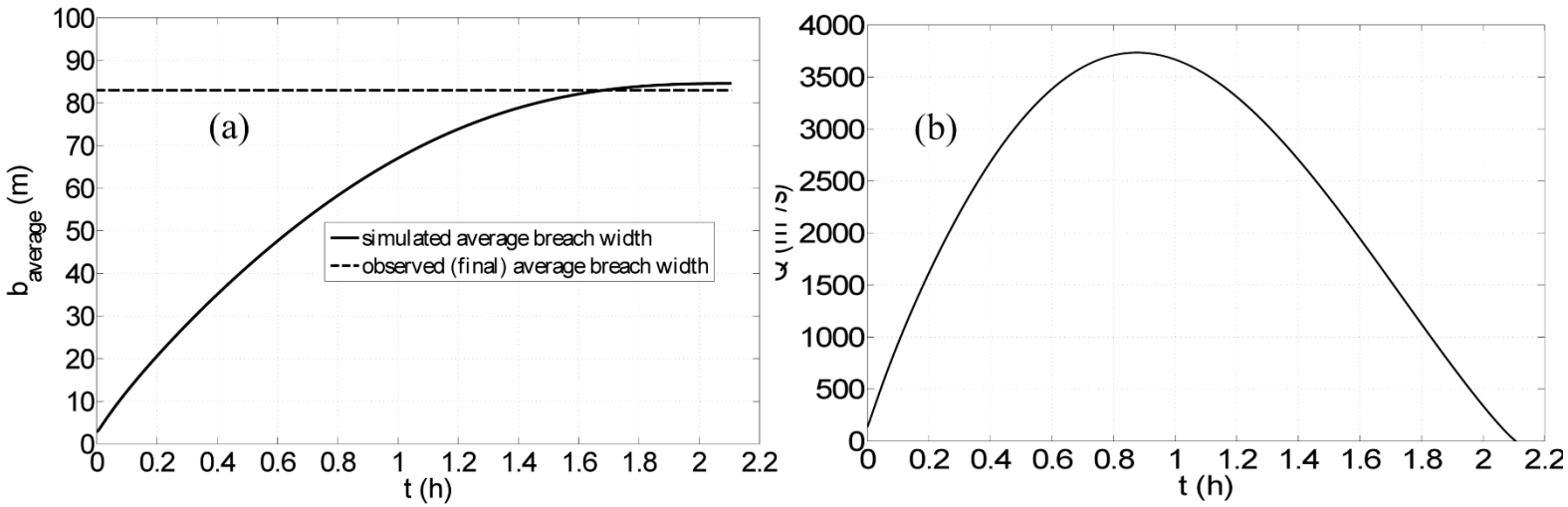

Figure 16. Simulation of the temporal behavior of both the mean breach width and the hydrograph using the Macchione (2008) model: v_e =0.09 m/s e tanβ=0.2 (M3 hydrograph)

Since M2 and M3 are based on observed data, they can be considered as two possible historical reconstructions of the event. M1 instead represents the results of the Macchione (2008) model used in a predictive mode, since it is based on the standard value suggested by Macchione (2008) for the parameter v_e. The most important results of the hydrographs are summarized in table 11.

Table 11. Simulated results obtained by the different version of the Macchione (2008) model

Hydrograph's ID	v_e (m/s)	tanβ	Simulated average breach width (m)	Error (%)	Duration of the simulated hydrograph (hr)	Peak discharge (m^3/s)
M1	0.07	0.2	75	-10	2.4	3,313
M2	0.07	0.955	88	6	2.2	3,497
M3	0.09	0.2	85	2	2.1	3,733

4.3.2 HEC-RAS dam breach computation

Besides the hydrographs computed using the Macchione (2008) model, in this part of thesis the hydrographs computed by Yochum et al. (2008), using the dam breach option within HEC-RAS, have been considered. The following information is taken from Yochum et al. (2008). The breach hydrograph was created with breach geometry measured primarily from aerial photography and breach formation time developed from Burge (2004). Breach progression was assumed to follow a sine wave. The breach formation time is estimated to be 55

min. Volume of the HEC-RAS developed breach hydrograph was 17,500,000 m^3, matching the estimated storage available at the time of failure with an initial water surface elevation of 84.89 m. The hydrograph used by Yochum et al. (2008) will be named HR. The authors computed also another two hydrographs which will be referred to here as FR and ML. They were obtained using the parameters provided using the formulas proposed by Froehlich (1995 a & b) and MacDonald and Langridge-Monopolis (1984), respectively. The main characteristics of the hydrographs are summarized in table 12.

Table 12. Information related to the numerical hydrographs used in the computations

Model	Hydrograph's ID	Assumed values for the parameters				Peak discharge (m^3/s)
		v_e (m/s)	Breach side slopes	Average breach width (m)	Breach formation time (h)	
Macchione (2008)	M1	0.07	0.2	-	-	3313
	M2	0.07	0.955	-	-	3497
	M3	0.09	0.2	-	-	3733
Hec-Ras+ Observation parameters	HR	-	1.3 & 0.6 (observed)	83.2 (observed)	0.92 (observed)	4160
Hec-Ras + Froehlich (1995 a,b) parameters	FR	-	0.9	61.5	1.7	2700
Hec-Ras+ MacDonald &Langridge-Monopolis (1984) parameters	ML	-	0.5	59.6	1	3130

4.4 1-D Flood propagation

An accurate 1-D numerical simulation of flood propagation was obtained by Yochum et al. (2008) using the hydrograph HR obtained with the dam breach module implemented in the well-known HEC-RAS software. This module is based on the parametric approach for the dam breach modelling. This requires, as input, the values of the final breach width and its developing time. In order to compare all the simulations, methods for measuring quantitative performance should be used (Bennett et al., 2013). In particular, we have considered the mean error, the mean absolute error and their standard deviation (SD). Considering the actual dam breach geometry, and inserting the Manning coefficient values estimated by visual inspection, Yochum et al. (2008) calculated water-surface elevations with an absolute average error of 0.34 m, with respect of measured high water marks. Using the same geometry and roughness coefficients considered by Yochum et al. (2008), we have obtained the results summarized in table 13 while, in table 14, the associated performances ranking is reported. The errors reported in table 13 can be considered very low, considering the fact that floods due to dam failure are characterized by very high water depths. For the HR hydrograph the error ranges between -0.90 m and +0.62 m; for the M1 hydrograph between -0.95 m and +0.55 m; for the M2 hydrograph between -0.85 m and +0.66 m; for the M3 hydrograph between -0.74 m and +0.77 m; for the FR hydrograph between -1.28 m and +0.41 m; for the ML hydrograph between

-1.07 m and +0.41 m. The mean error values are also very low. Among all the computed hydrographs, the M3 hydrograph gives the closest value of the mean error to zero, followed by the M2, M1 and HR ones. The FR and ML hydrographs show a tendency to underestimate the maximum water surface elevations. In terms of absolute error, the best results have been achieved by the HR hydrograph (0.34 m), followed by M3 (0.39 m), M2 (0.40 m), M1 (0.41 m), ML (0.45 m) and FR (0.49 m).

Table 13. 1-D flood propagation results

River Sta	Distance (km)	Observed W.M.E. (m a.s.l.)	Water marks ID	Min Ch El (m)	HR(*)			M1			M2			M3			FR			ML		
					Q (m3/s)	W.S.E. (m a.s.l.)	Error (m)	Q (m3/s)	W.S.E. (m a.s.l.)	Error (m)	Q (m3/s)	W.S.E. (m a.s.l.)	Error (m)	Q (m3/s)	W.S.E. (m a.s.l.)	Error (m)	Q (m3/s)	W.S.E. (m a.s.l.)	Error (m)	Q (m3/s)	W.S.E. (m a.s.l.)	Error (m)
496048.*	1.148	75.07	21	67.97	4030	75.08	0.01	3279	74.64	-0.43	3457	74.75	-0.32	3691.5	74.89	-0.18	2761	74.29	-0.78	3079	74.5	-0.57
495418	1.313	74.92	17	67.12	4020	74.33	-0.59	3277	73.97	-0.95	3454	74.07	-0.85	3689	74.18	-0.74	2759	73.67	-1.25	3074.8	73.85	-1.07
494416.*	1.616	73.49	20	66.14	3940	72.91	-0.58	3253	72.57	-0.92	3429	72.66	-0.83	3657	72.78	-0.71	2735	72.21	-1.28	3035	72.42	-1.07
493621.*	1.858	73.03	18	65.94	3930	72.43	-0.6	3240	72.12	-0.91	3415	72.21	-0.82	3641	72.33	-0.7	2727	71.82	-1.21	3023	71.97	-1.06
489003	3.266	69.19	23-25	60.84	3020	69.81	0.62	2869	69.74	0.55	3002	69.85	0.66	3151	69.96	0.77	2395	69.31	0.12	2473	69.37	0.18
480714	5.792	66.45	27	57.18	2290	66.52	0.07	2291	66.52	0.07	2370	66.61	0.16	2456	66.71	0.26	2004	66.19	-0.26	2021	66.22	-0.23
480601	5.826	65.86	26&29	57.18	2550	65.54	-0.32	2620	65.62	-0.24	2732	65.7	-0.16	2845	65.77	-0.09	2145	65.24	-0.62	2178	65.27	-0.59
474299	7.747	63.09	19	55.47	2100	63.46	0.37	2332	63.61	0.52	2424	63.66	0.57	2479	63.69	0.6	1854	63.27	0.18	1871	63.28	0.19
471891	8.48	62.36	16	53.34	1970	62.34	-0.02	2186	62.56	0.2	2259	62.62	0.26	2305	62.65	0.29	1764	62.17	-0.19	1778	62.18	-0.18
461552	11.627	59.04	41	49.77	1470	59.12	0.08	1712	59.28	0.24	1771	59.33	0.29	1773	59.32	0.28	1398	58.98	-0.06	1404	58.99	-0.05
450426	15.018	55.66	40	46.79	1150	54.76	-0.9	1302	55.03	-0.63	1336	55.09	-0.57	1324	55.06	-0.6	1135	54.74	-0.92	1137	54.74	-0.92
435769	19.486	50.81	39	41.76	978	50.93	0.12	1109	51.14	0.33	1139	51.18	0.37	1123	51.16	0.35	978	50.93	0.12	979	50.93	0.12
408806	27.703	43.1	32&33	35.05	797	42.95	-0.15	883	43.16	0.06	910	43.21	0.11	889	43.17	0.07	803	42.97	-0.13	803	42.97	-0.13
406278	28.474	42.39	34&37	34.35	784	42.05	-0.34	868	42.29	-0.1	891	42.35	-0.04	874	42.3	-0.09	790	42.07	-0.32	791	42.07	-0.32
406278	28.474	42.43	38	34.35	784	42.05	-0.38	868	42.29	-0.14	891	42.35	-0.08	874	42.3	-0.13	791	42.07	-0.36	791	42.07	-0.36
406117	28.523	42.09	35&36	34.35	781	41.76	-0.33	865	41.91	-0.18	888	41.95	-0.14	870	41.92	-0.17	788	41.77	-0.32	788	41.77	-0.32
398757	30.766	38.92	9	33.38	770	39.32	0.4	843	39.45	0.53	865	39.48	0.56	848	39.46	0.54	769	39.33	0.41	769	39.33	0.41
398594	30.812	38.8	7	33.38	762	39.07	0.27	846	39.19	0.39	865	39.22	0.42	848	39.19	0.39	769	39.08	0.28	769	39.08	0.28

(*) Results by Yochum et al. (2008)

Table 14. Performances of the numerical hydrographs sorted by absolute error

Simulation 1-D	Absolute error (m)		Error (m)	
	Mean	SD	Mean	SD
HR	0.34	0.25	-0.13	0.41
M3	0.39	0.25	0.01	0.47
M2	0.4	0.27	-0.02	0.49
M1	0.41	0.29	-0.09	0.51
ML	0.45	0.35	-0.32	0.48
FR	0.49	0.42	-0.37	0.53

The hydrograph obtained using the three versions of the Macchione (2008) model gave very similar results. In order to evaluate the accuracy of the results throughout the downstream valley, the errors have been computed subdividing the domain into two parts. In particular, the HWM dataset has been split into two parts, dividing by two the total number of HWM, so that we separated the points belonging to the upstream and downstream areas of the domain. The results are reported in tables 15 and 16. Upstream, the best result has been provided by the HR hydrographs, in terms of absolute error, and by the M3 one in terms of mean error. Therefore, the analysis of HWM upstream confirmed the ranking of the total dataset discussed above. Downstream, the best results have been obtained

using M2, M1 and M3, followed by ML, FR and HR. All the hydrographs gave very similar results downstream.

Table 15. 1-D simulation results for the upstream 50% of water elevations

Simulation 1-D	Upstream HWM			
	(21, 17, 20, 18, 23-25, 27, 26-29,19, 16)			
	Error (m)		Absolute error (m)	
	Mean	SD	Mean	SD
HR	-0.116	0.44	0.353	0.262
M3	-0.056	0.577	0.482	0.272
M2	-0.148	0.599	0.514	0.292
M1	-0.234	0.606	0.532	0.333
ML	-0.489	0.511	0.571	0.404
FR	-0.588	0.581	0.654	0.494

Table 16. 1-D simulation results for the downstream 50% of water elevations

Simulation 1-D	Downstream HWM			
	(41, 40, 39, 32-33, 34-37, 38, 35-36, 9, 7)			
	Error (m)		Absolute error (m)	
	Mean	SD	Mean	SD
M2	0.102	0.35	0.287	0.205
M1	0.056	0.36	0.289	0.197
M3	0.071	0.357	0.291	0.194
ML	-0.143	0.399	0.323	0.255
FR	-0.144	0.399	0.324	0.254
HR	-0.137	0.401	0.33	0.244

4.4.1 Bridge effects

As is well-known, bridges might influence the water surface profile in a river during a flood event. Moreover, it has been recently observed that they can induce 2-D effects even in straight reach along which the suitability of 1-D approaches is generally accepted (Costabile & Macchione, 2015; Costabile et al., 2014, 2015). In this study, the bridge effect has been analyzed using the same HEC-RAS project but removing the bridges previously considered (see table 17). This evaluation has been carried out using only the HR hydrograph. The results obtained with bridges are very similar to those computed by Yochum et al. (2008). The absolute error, equal to 0.34 m in the simulation with bridges (HR), becomes 0.38 m removing the bridges (HR-WB). The mean error is -0.098 m for HR and -0.212 m for HR-WB. The maximum difference in the computation of water surface elevations between HR and HR-WB is -0.81 m and it is located just upstream of the Roadway Bridge (River Station 480714). All in all, according to HEC-RAS computation it seems that the bridges had a limited influence on the flood flow probably due to the limited narrowing induced by piers located in the riverbed. Actually, the ratio between the total width of the piers and transversal length of the bridge ranges from 2 % (Chaney Church Roadway Bridge) to 7 % (Columbia-Purvis Roadway Bridge).

Table 17. 1-D simulation results statistical analysis for the downstream 50% of water elevations

River Sta	Distance (km)	Observed W.M.E. (m a.s.l.)	Water marks ID	Min Ch El (m a.s.l.)	Simulation with bridges			Simulation without bridges			Error1-Error2 (m)
					Q (m3/s)	W.S.E. (m a.s.l.)	Error1 (m)	Q (m3/s)	W.S.E. (m a.s.l.)	Error2 (m)	
496048.*	7.13	75.07	21	67.97	4080	75.11	0.04	4080	74.93	-0.14	-0.18
495418	7.3	74.92	17	67.12	4071	74.36	-0.56	4059	74.01	-0.91	-0.35
495360	7.3	Columbia-Purvis Roadway Bridge									
494416.*	7.6	73.49	20	66.14	4000	72.93	-0.56	3999	72.93	-0.56	0
493621.*	7.84	73.03	18	65.94	3983	72.45	-0.58	3981.38	72.45	-0.58	0
489003	9.25	69.19	23-25	60.84	3061	69.84	0.65	3047	69.81	0.62	-0.03
488950	9.25	Salt Dome Roadway Bridge									
480714	11.78	66.45	27	57.18	2312	66.55	0.1	2539	65.74	-0.71	-0.81
480665	11.78	Chaney Church Roadway Bridge									
480601	11.81	65.86	26&29	57.18	2589	65.58	-0.28	2530	65.55	-0.31	-0.03
474299	13.73	63.09	19	55.47	2158	63.49	0.4	2194	63.08	-0.01	0.39
471950	14.37	Luther Saucier Roadway Bridge									
471891	14.47	62.36	16	53.34	2016	62.38	0.02	2036	62.42	0.06	0.04
461620	17.61	Pinebur Roadway Bridge (upper)									
461552	17.61	59.04	41	49.77	1511	59.08	0.04	1611	59.18	0.14	0.1
450426	21	55.66	40	46.79	1174	54.8	-0.86	1238	54.91	-0.75	0.11
435769	25.47	50.81	39	41.76	1001	50.97	0.16	1038	50.88	0.07	-0.09
435695	25.47	Pinebur Roadway Bridge (lower)									
408806	33.69	43.1	32&33	35.05	812	42.99	-0.11	837	42.97	-0.13	-0.02
406278	34.46	42.39	34&37	34.35	799	42.09	-0.3	821	41.93	-0.46	-0.16
406278	34.46	42.43	38	34.35	799	42.09	-0.34	821	41.93	-0.5	-0.16
406200	34.46	MS-13 Roadway Bridge									
406117	34.54	42.09	35&36	34.35	796	41.79	-0.3	819	41.83	-0.26	-0.04
398757	36.75	38.92	9	33.38	776	39.34	0.42	796	39.21	0.29	-0.13
398675	36.75	MS-43 Roadway Bridge									
398594	36.8	38.8	7	33.38	776	39.09	0.29	796	39.12	0.32	0.03
		Mean error					-0.13			-0.21	
		Mean absolute error					0.34			0.38	
		Standard deviation (error)					0.41			0.42	
		Standard deviation (absolute error)					0.25			0.27	

4.5 2-D Flood propagation

A first study related to the 2-D flood propagation has been presented by Altinakar et al. (2010), who used the shallow water equations solved using a first order finite-volume upwind method. They used a structured mesh and the element side was equal to 20 m. The computational domain was obtained starting from a 10 *m* DEM, available at Mississippi Automated Resource Information System (MARIS). A constant value (0.05 $m^{-\frac{1}{3}}s$) throughout the domain was used for the Manning coefficient. The authors did not consider the bridges in their simulation. The hydrograph flowing through the breach was computed using the same final breach geometry assumed by Yochum et al. (2008). In order to obtain the same discharge peak as Yochum et al. (2008), by a trial and error procedure they assumed the breaching duration equal to 38 minutes, obtaining a discharge peak value equal to 4155 m^3/s. On the basis of the authors experience in the performance of flood propagation models (Costabile et al., 2012), in this part of thesis, the 2-D simulation has been performed using a numerical code based on the fully dynamic shallow water equations applied to a computational domain composed of an unstructured grid with irregular triangular elements. The mathematical model is based on the 2-D shallow water equations (SWE) that can be expressed in the following form:

$$\frac{\partial U}{\partial t}+\frac{\partial F}{\partial x}+\frac{\partial G}{\partial y}=S \tag{4.1}$$

where:

$$U=\begin{pmatrix} h \\ hu \\ hv \end{pmatrix};\quad F=\begin{pmatrix} hu \\ hu^2+gh^2/2 \\ huv \end{pmatrix};\quad G=\begin{pmatrix} hv \\ huv \\ hv^2+gh^2/2 \end{pmatrix};\quad S=\begin{pmatrix} q \\ gh\left(S_{0x}-S_{fx}\right) \\ gh\left(S_{0y}-S_{fy}\right) \end{pmatrix}$$

in which: t is time; x, y are the horizontal coordinates; h is the water depth; u, v are the depth-averaged flow velocities in x- and y- directions, respectively; g is the gravitational acceleration; S_{0x}, S_{0y} are the bed slopes in x- and y- directions; S_{fx}, S_{fy} are the friction slopes in x- and y- directions; q is a lateral inflow. For the numerical integration of system (1), in this thesis the finite volume methodology (FVM) has been used. All the details about the numerical flux and source terms computations, wet-dry treatment and grid generation process can be found in Costabile and Macchione (2015) and it is not reported here for the sake of brevity. The analysis discussed here is based on a 10 m Digital Elevation Model, available at the National Map Viewer provided by USGS (United States, Geological Service). The elevation data, composing the National Elevation Dataset, have been published using different spatial resolutions. The studied area is covered only in part by the 3 m DEM and, for this reason, the analysis presented here has been carried out using only the 10 m DEM. In particular, the data refer to a survey performed in 1999 and are available in NAD1983 reference system. The upstream boundary condition is represented by the hydrographs synthetically reported in table 12. The downstream boundary condition has been

set according to the flow regime: transmissive boundary condition for supercritical flow and critical flow for subcritical condition. In reality, the boundary cells are located very far (more than 2 km) from the last water marks and, consequently, the effects of the physical condition imposed there have no particular influences on the results. As already performed by Altinakar et al. (2010), the simulation has been carried out without inserting the bridges. The numerical results obtained using the 2-D modelling are summarized in table 18. First of all, it should be observed that some HWM elevations are lower than the bed elevations (see HWM number 33, 34, 10 and 11). This fact might be induced by an uncertainty in the high marks measurements or in the DEM used. Neglecting those water marks for which the simulations have predicted a dry bed, the errors range from -1.6 m and +0.8 m. The performances of each simulation are summarized in table 19.

Table 18. 2-D simulation results

Water marks No.	Observed W.S.E. (m a.s.l)	Bed elevation	M1		M2		M3		HR		ML		FR	
			W.S.E (m a.s.l)	Error (m)	W.S.E (m a.s.l)	Error (m)	W.S.E (m a.s.l)	Error (m)	W.S.E (m a.s.l)	Error (m)	W.S.E (m a.s.l)	Error (m)	W.S.E (m a.s.l)	Error (m)
21	75.07	74.38	74.38	-0.69	74.38	-0.69	74.39	-0.68	74.4	-0.67	74.38	-0.69	74.38	-0.69
17	74.92	73.2	73.3	-1.62	73.33	-1.59	73.38	-1.54	73.47	-1.45	73.27	-1.65	73.24	-1.68
22	72.33	70.71	70.73	-1.6	70.77	-1.56	70.79	-1.54	70.79	-1.54	70.71	-1.62	70.71	-1.62
20	73.49	72.42	72.52	-0.97	72.57	-0.92	72.62	-0.87	72.73	-0.76	72.49	-1	72.46	-1.03
18	73.03	71.95	72.02	-1.01	72.04	-0.99	72.09	-0.94	72.19	-0.84	72	-1.03	71.98	-1.06
23	69.19	68.28	68.45	-0.74	68.49	-0.7	68.53	-0.66	68.49	-0.7	68.37	-0.83	68.36	-0.83
28	65.75	63.72	65.06	-0.69	65.12	-0.63	65.19	-0.56	65.05	-0.7	64.78	-0.97	64.79	-0.96
29	65.75	63.59	65.03	-0.72	65.09	-0.66	65.16	-0.59	65.02	-0.73	64.73	-1.02	64.73	-1.02
27	66.45	64.55	65.3	-1.15	65.34	-1.11	65.38	-1.07	65.3	-1.15	65.12	-1.33	65.12	-1.33
26	65.96	65.33	65.48	-0.48	65.51	-0.45	65.54	-0.42	65.48	-0.48	65.4	-0.56	65.4	-0.56
16	62.36	60.56	62.17	-0.19	62.2	-0.16	62.23	-0.13	62.08	-0.28	61.93	-0.43	61.94	-0.42
41	59.07	57.09	58.81	-0.26	58.83	-0.24	58.84	-0.23	58.67	-0.4	58.59	-0.48	58.6	-0.47
42	59.13	58.43	59.11	-0.02	59.14	0.01	59.16	0.03	58.99	-0.14	58.93	-0.2	58.93	-0.2
40	55.66	55	55.57	-0.09	55.58	-0.08	55.6	-0.06	55.41	-0.25	55.35	-0.31	55.36	-0.3
39	50.81	47.02	50.69	-0.12	50.69	-0.12	50.71	-0.11	50.5	-0.31	50.48	-0.33	50.48	-0.33
33	43.07	43.95	43.95	0.88	43.95	0.88	43.95	0.88	43.95	0.88	43.95	0.88	43.95	0.88
32	43.13	42.79	42.87	-0.26	42.87	-0.26	42.87	-0.26	42.83	-0.3	42.83	-0.3	42.83	-0.3
37	42.49	40.02	42.1	-0.39	42.11	-0.38	42.12	-0.37	41.88	-0.61	41.88	-0.61	41.88	-0.61
38	42.43	41.68	42.04	-0.39	42.05	-0.38	42.05	-0.38	41.91	-0.52	41.91	-0.52	41.91	-0.52
36	42.06	40.18	41.45	-0.61	41.46	-0.6	41.47	-0.59	41.27	-0.79	41.26	-0.8	41.26	-0.8
35	42.12	41.28	41.74	-0.38	41.74	-0.38	41.75	-0.37	41.65	-0.47	41.64	-0.48	41.65	-0.47
34	42.28	42.44	42.44	0.16	42.44	0.16	42.44	0.16	42.44	0.16	42.44	0.16	42.44	0.16
10	38.62	38.81	39.1	0.48	39.1	0.48	39.11	0.49	39.02	0.4	39.01	0.39	39.01	0.39
9	38.92	36.92	38.28	-0.65	38.28	-0.64	38.28	-0.64	38.2	-0.72	38.2	-0.72	38.2	-0.72
11	38.47	39.31	39.32	0.85	39.32	0.85	39.32	0.85	39.31	0.84	39.31	0.84	39.31	0.84
8	38.68	36.69	38.23	-0.45	38.23	-0.45	38.24	-0.44	38.16	-0.52	38.16	-0.52	38.16	-0.52
14	38.89	36.79	38.78	-0.11	38.78	-0.11	38.79	-0.1	38.69	-0.2	38.69	-0.2	38.69	-0.2
13	38.89	36.29	38.75	-0.14	38.75	-0.14	38.75	-0.14	38.66	-0.23	38.66	-0.23	38.66	-0.23
7	38.8	34.69	38.66	-0.14	38.66	-0.14	38.67	-0.13	38.57	-0.23	38.57	-0.23	38.57	-0.23
6	38.77	36.33	38.61	-0.16	38.61	-0.16	38.61	-0.16	38.52	-0.25	38.52	-0.25	38.52	-0.25
4	38.74	37.29	38.51	-0.23	38.51	-0.23	38.51	-0.23	38.42	-0.32	38.42	-0.32	38.42	-0.32
5	38.74	37.75	38.55	-0.19	38.55	-0.19	38.56	-0.18	38.47	-0.27	38.47	-0.27	38.47	-0.27
3	38.71	37.76	38.44	-0.27	38.44	-0.27	38.45	-0.26	38.37	-0.34	38.36	-0.35	38.37	-0.34
1	38.71	37.63	38.42	-0.29	38.42	-0.29	38.43	-0.28	38.34	-0.37	38.34	-0.37	38.34	-0.37
2	38.74	37.7	38.43	-0.31	38.43	-0.31	38.43	-0.31	38.35	-0.39	38.35	-0.39	38.35	-0.39

Table 19. Statistics related to the 2-D propagation of the flood hydrographs (simulation without bridges)

2-D Simulation without bridges	Absolute error (m)		Error (m)	
	Mean	SD	Mean	SD
M3	0.476	0.385	-0.338	0.514
M2	0.492	0.396	-0.356	0.525
M1	0.505	0.405	-0.37	0.535
HR	0.548	0.342	-0.418	0.496
ML	0.608	0.391	-0.478	0.546
FR	0.609	0.396	-0.48	0.55

All the simulations are characterized by a negative mean error. The lowest error is equal to 0.34 m, provided by the simulation with the M3 hydrograph. The highest error is equal to -0.48 m, obtained by the simulation with the FR hydrograph. The presented ranking has been organized according to the mean error values and it is the same as the absolute error. The lowest errors have been achieved by using the M3 hydrograph, calibrated in order to have the simulated final mean breach equal to the observed one. The simulation based on the M2 hydrograph, calibrated in order to have the same mean side slope of the breach, is in second position while the M1 hydrograph, that is the Macchione (2008) model with the standard value of the parameters, is in third position. The list ends with the HR, ML and FR hydrographs. The negative sign of the mean error

highlights that all the simulations have underestimated the observed values. This effect might be induced by the roughness coefficient assumed in the computations and, for this reason, another run of the HR hydrograph has been performed. In particular, the roughness value has been set to 0.07 $m^{-\frac{1}{3}}s$ from 0.05 $m^{-\frac{1}{3}}s$.

Table 20. Influence of the roughness values on the 2-D propagation results (HR hydrograph)

2-D Simulation without bridges	Absolute error (m)		Error (m)	
	Mean	SD	Mean	SD
HR, n =0.05 $m^{-\frac{1}{3}}s$	0.54	0.36	-0.41	0.5
HR, n =0.07 $m^{-\frac{1}{3}}s$	0.49	0.27	-0.37	0.43

The results, reported in table 20, show that the increase in the roughness value only lead to a slight reduction of the mean error and the standard deviation. Moreover, the effect of the bridges that have not been considered in the above presented computations should be checked. The bridge influence has been taken into account only by the insertion of the bridge abutments because the

obstruction induced by piers is very limited. The results are summarized in table 21.

Table 21. Statistics related to the 2-D propagation of the flood hydrographs (simulation with bridges)

2-D Simulation with bridges	Absolute error (m)		Error (m)	
	Mean	SD	Mean	SD
M3	0.47	0.39	-0.27	0.54
M2	0.49	0.39	-0.29	0.56
M1	0.51	0.4	-0.31	0.57
HR	0.53	0.33	-0.34	0.53
ML	0.61	0.39	-0.42	0.59
FR	0.61	0.4	-0.45	0.6

The mean error is lower than the simulation with bridges but just by a few centimeters, confirming the fact that bridges narrowing influence is very low. The absolute error is practically the same as before. Moreover, the ranking of the results related to the hydrographs used still holds. Once again, the lowest errors have been obtained using the M3 hydrographs. In conclusion, the 2-D computations have highlighted absolute errors between 0.5-0.6 m and mean errors ranging from -0.5 m to -0.3 m. They are comparable to those obtained by Altinakar et al. (2010) using a 20 m DEM. The mean errors values have been

slightly influenced by inserting the bridge abutments or by increasing the roughness and, therefore, we can conclude that the roughness values estimations are good enough for this case and that the bridges have not influenced significantly the simulation. For the event considered here, it seems that the sources of uncertainties are mainly limited to the topographic data or to phenomena not explicitly considered here like debris transport or morphological bed variations. Anyway, the results can be considered satisfactory in terms of prediction of the event. Finally, in order to evaluate the trend of the performances throughout the valley, the errors have been computed separating the upstream points from the downstream ones. The results are presented in tables 22 and 23.

Table 22. 2-D simulation results for the upstream 50% of water elevations

Upstream HWM (21, 17, 22, 20, 18, 23-25, 28, 29, 27, 26, 16, 41, 42, 40, 39, 33, 32)				
	Error (m)		Absolute error (m)	
	Media	SD	Media	SD
M3	-0.515	0.597	0.622	0.477
M2	-0.546	0.608	0.651	0.487
M1	-0.572	0.618	0.676	0.494
HR (n =0.05)	-0.577	0.553	0.681	0.408
ML	-0.698	0.606	0.801	0.449
FR	-0.701	0.613	0.805	0.457

Table 23. 2-D simulation results for the downstream 50% of water elevations

Upstream HWM (21, 17, 22, 20, 18, 23-25, 28, 29, 27, 26, 16, 41, 42, 40, 39, 33, 32)				
	Error (m)		Absolute error (m)	
	Media	SD	Media	SD
M3	-0.172	0.363	0.338	0.204
M2	-0.177	0.364	0.342	0.204
M1	-0.178	0.364	0.343	0.204
HR (n =0.05)	-0.268	0.395	0.422	0.207
ML	-0.27	0.396	0.425	0.207
FR	-0.27	0.396	0.425	0.207

For both the data sets, the best result has been achieved by the M3 hydrograph, followed by M2, M1, HR, ML and FR. Therefore, the ranking discussed above has been confirmed also by this kind of analysis. The maximum water levels simulated by the 2-D model based on the M1 hydrograph are shown in figure 17 while, in figure 18, the evolution of flood propagation is depicted.

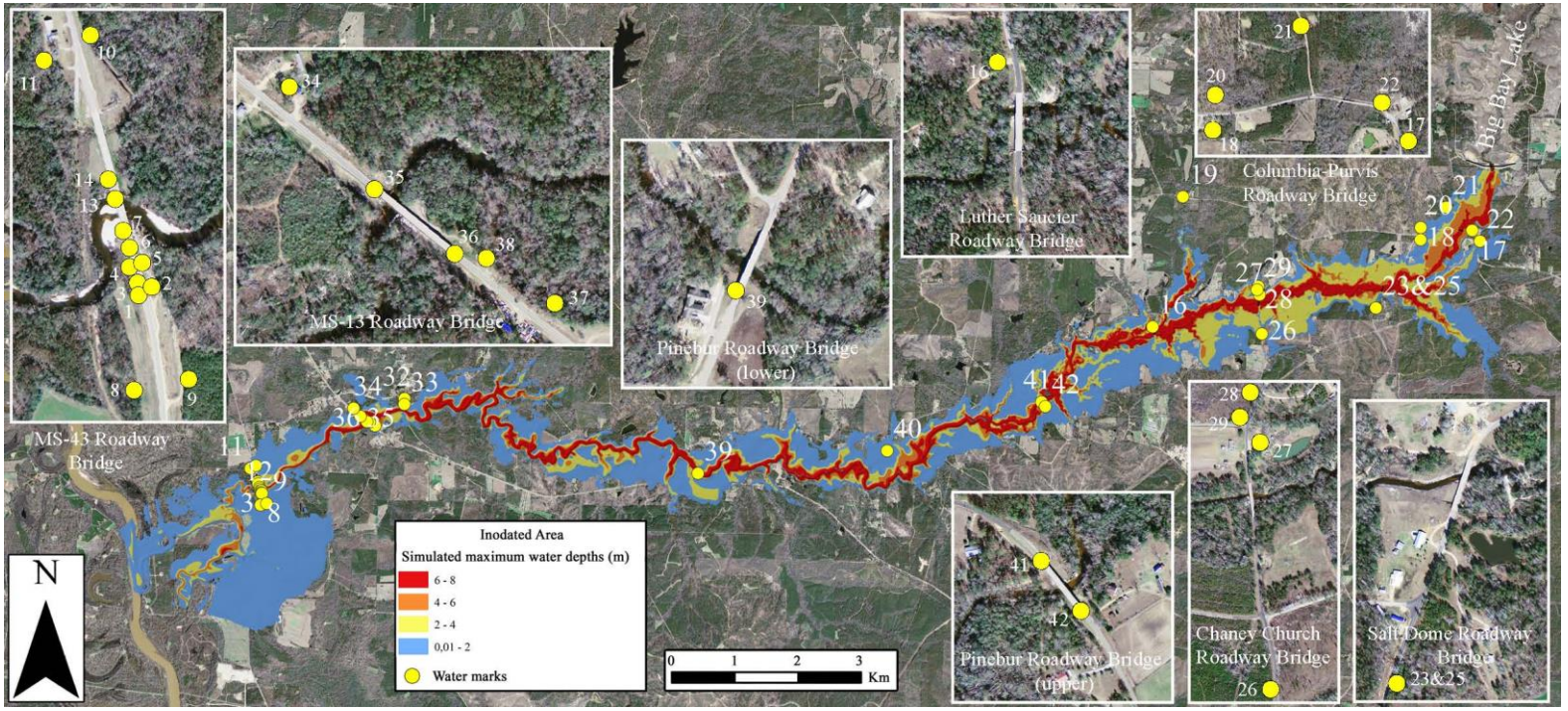

Figure 17. Maximum water depths simulated using the Macchione (2008) model (M1 hydrograph, 2-D simulation)

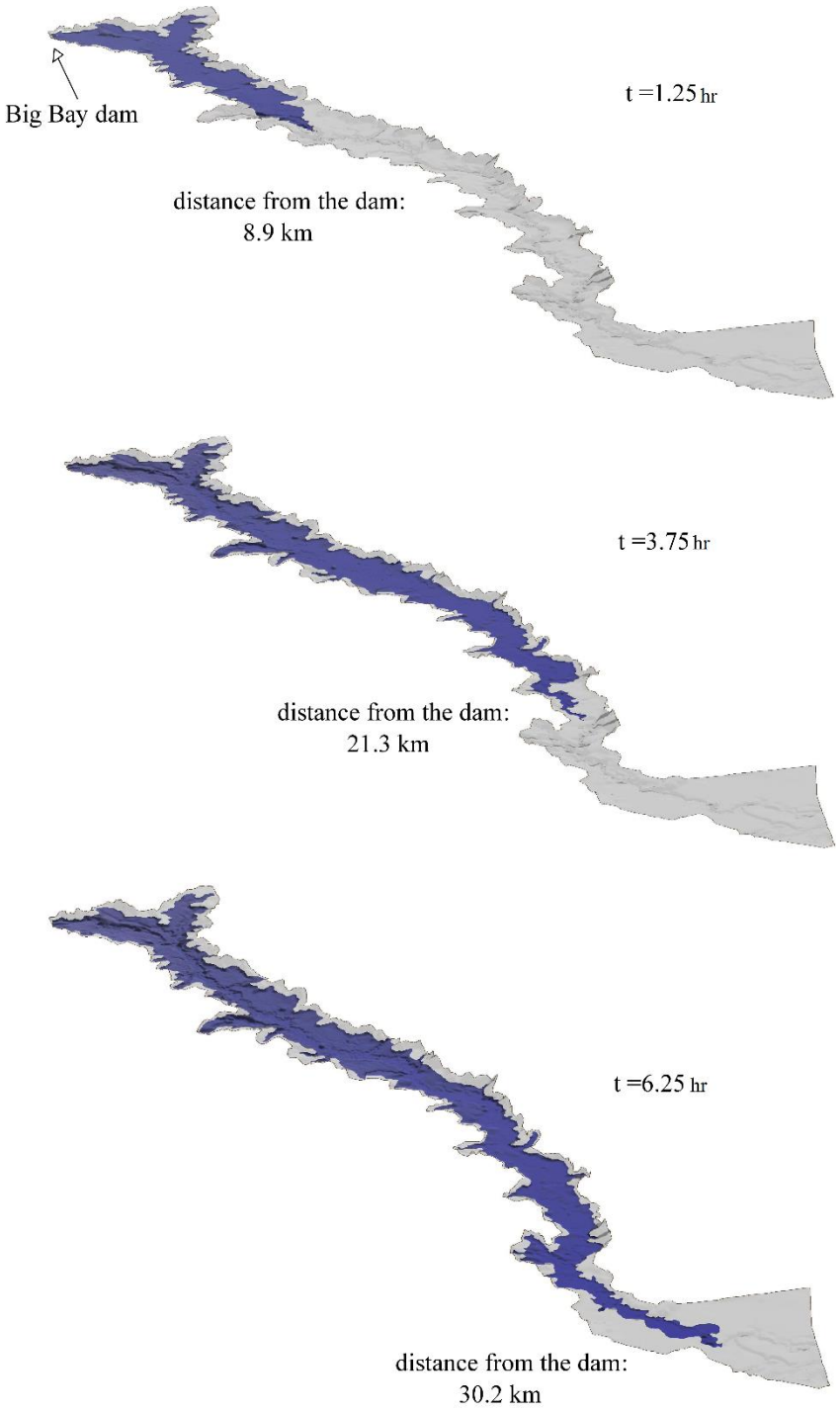

Figure 18. Flood propagation evolution simulated using the Macchione (2008) model (M1 hydrograph)

Conclusions

This thesis has focused on two aspects related to accuracy aspects in dam breach studies: a suitable analytical relation for the description of the morphology of the reservoir and the influence exerted by the methods used for computing the dam breach hydrograph on the simulated maximum water levels throughout the valley downstream of a dam. Regarding the first aspect, the first part of this thesis showed that the morphology of river reservoirs can be represented with very good accuracy, using Eq. (3.1). This finding has been verified for lakes that have a very large variability of planimetric shapes, belonging to 3 different regions of the world. Eq. (3.1) has the merit of being very simple, so its use gives many advantages. In particular it only requires the calculation of 2 parameters (W_0 and α_0). Moreover, in this thesis it has been shown that even for reservoirs for which few points in the elevation-volume curve are available, Eq. (3.1) provides an accurate representation of the morphology of the reservoir. This is still true if only two points in the curve can be used. Even when the area and volume are available for only a single point Z taken in the upper part of the reservoir, it is possible to calculate the parameters of Eq. (3.1), by using Eqs.

(3.5) and (3.6). In this case errors may be higher for the lower part of the curve, though, all the methods proposed for the approximation of the morphology of the reservoir gave very accurate results in dam breach calculations. The simplicity of the formula is particularly useful for systematic studies in dam breach, as these studies are best carried out using dimensionless models (see De Lorenzo and Macchione (2010 & 2014), Macchione (1986 & 1989) and Macchione and Rino (2008)). In particular, using the non dimensional formulation of the model, the parameters of Eq. (3-1) are reduced to one (α_0). The exponent α_0 has a precise morphological meaning, as it describes, with a simple numeric value, the degree of flaring of the reservoir. So, as has been said above, the remarkable influence of the reservoir flaring on the results of dam breach calculations, can be easily explored simply by varying the parameter α_0.

Another novelty of this study raised from lacking significant contribution for selecting the most suitable dam breach model to be used in flood mapping studies and, consequently, to be implemented in common flood propagation software. For this reason, the analysis has been carried out focusing on the water levels of the flow propagating downstream. To achieve this purpose, in the second part of the thesis the Big Bay dam failure has been considered, for which not only observed breach data but also high water marks throughout the valley are available. Following the work by Yochum et al. (2008), the parametric models have been considered which are, nowadays, the ones most used in the

commercial software. Moreover, they are easier to use than more complex models based on geotechnical or geometrical relationships for assessing the stability of breach sides, which show an important drawback for technical studies since they have a lot of parameters whose estimation increases the global uncertainty of the entire modelling chain (generation and propagation of the hydrograph). Together with the parametric model, the Macchione (2008) model has been used for its remarkable predictive ability and its ease of use. Regarding the flood propagation modelling, this research has been carried out using HEC-RAS as a 1-D approach and a finite volume method based on an unstructured grid recently proposed by Costabile and Macchione (2015) for the 2-D analysis. Six hydrographs have been considered in this work. The first three have been simulated using HEC-RAS and the same river model considered by Yochum et al. (2008) in order to make the comparison easier. For the breach parameters, the authors used observed data (the HR hydrograph), and those obtained using the formulas proposed by Froehlich (1995 a & b) (the FR hydrograph) and MacDonald and Langridge-Monopolis (1984) (the ML hydrograph). The Macchione (2008) model has been used in three different ways: the first one is based on the values of the parameters proposed by the author in his original work, so that the model is intended to work in a predictive mode. In the other two options, one parameter has been set *ad hoc*. The comparison between the simulated maximum water levels and the observed HWM shows a substantial

similitude among the results obtained using the different hydrographs. Despite the uncertainties due to the topography used for the generation of the Digital Elevation Model, the absolute errors in terms of simulated maximum water levels, obtained using all the hydrographs, are quite limited if compared with the high water depths that characterize the event. For the 1-D calculations, the lowest absolute error has been obtained using the HR hydrograph, while the lowest mean value has been obtained using the M3 hydrograph. However, it should be observed that the HR hydrograph has been computed inserting the historical observed data and the M3 one has been obtained by setting ad hoc one parameter of the Macchione (2008) model in order to have the final mean breach width equal to the observed one. For predictive purposes, Yochum et al. (2008) have estimated some breach parameters using the Froehlich (1995 a & b) and MacDonald and Langridge-Monopolis (1984) formulas. This approach gave less accurate results than those obtained using the M1 hydrograph, i.e. the Macchione (2008) model used in a predictive mode. It might be important to underline that the hydrographs have shown different peak values. For example, the use of HR and M3 hydrographs has provided similar results in terms of simulated water levels but they are characterized by different values of peak discharge, 4160 and 3733 m^3/s respectively. It is interesting to note that although the HR hydrograph simulated a higher peak value than the M3 hydrograph (a difference up to 427 m^3/s), the latter seems to provide less underestimation of the maximum water

levels than the HR hydrograph. As for the 2-D modelling results, the best numerical reconstruction of the event has been provided by the M3 hydrograph while the most accurate prediction has been obtained by the M1 hydrograph. The simulation results based on the M1 hydrograph have been even better than those obtained using the HR hydrograph in which, as already recalled, the historical data have been inserted as input. For this reason, the results presented here allow one to underline an important conclusion. In its predictive mode (the M1 hydrograph), that means the no calibration parameter has to be tuned because the suggested values are used, the Macchione (2008) model has provided reliable and similar, at least or even better, results to those ones that can be simulated using the parametric models, which need the estimation of some parameters that can add further uncertainties in studies like these. Therefore, the analysis carried out in this work suggests that the Macchione (2008) model can be effectively nested in the flood propagation software, to support or substitute those currently used, for three reasons at least: its predictive ability, the absence of calibration parameter to be set *ad hoc* and the ease of use.

Bibliography

Abdullah, A. F., Vojinovic, Z., Price, R. K., & Aziz, N. A. A. (2012). Improved methodology for processing raw LIDAR data to support urban flood modelling - accounting for elevated roads and bridges. *Journal of Hydroinformatics, 14*(2), 253-269.

Altinakar, M. S., McGrath, M. Z., Ramalingam, V. P., & Omari, H. (2010, 8-10 Settembre). *2D modelling of Big Bay Dam failure in Mississippi: Comparison with field data and 1D model results.* Paper presented at the River Flow 2010 – Proceedings of International Conference on Fluvial Hydraulics, Braunschweig, Germany.

ASCE/EWRI. (2011). Earthen Embankment Breaching. *Journal of Hydraulic Engineering, 137*(12), 1549-1564.

Balloffet, A., & Scheffler, M. L. (1982). Numerical analysis of the Teton Dam failure flood. *Journal of Hydraulic Resource, 20*(4), 317–328.

Bennett, N. D., Croke, B. F. W., Guariso, G., Guillaume, J. H. A., Hamilton, S. H., Jakeman, A. J., Andreassian, V. (2013). Characterising performance of environmental models. *Environmental Modelling & Software, 40*, 1-20.

Benoist, G., & Nicollet, G. (1983). *Rupture progressive des barragesen terre.* Paper presented at the Proc. 20th IAHR Congress, Moscow.

Broich, K. (2002). Description of the parameter model DEICH-P *Tech. Report*: University of the Federal Armed Forces Munich.

Burge, T. R. (2004). *Big Bay Dam: Evaluation of failure, Land Partners Limited Partnership*. Hattiesburg, MS.

Cao, Z. X., Yue, Z. Y., & Pender, G. (2011). Landslide dam failure and flood hydraulics, Part II: coupled mathematical modelling. *Natural Hazards, 59*(2), 1021-1045.

Chadwick, W. L., Casagrande, A., Coombs, H. A., Dowd, M. W., Fucik, E. M., Higginson, R. K., Jamsen, R. B. (1976). Failure of teton dam. Idaho falls, Idaho: U. S. department of the interior and state of Idaho.

Chanson, H. (2004). Discussion of Overtopping breaching of noncohesive homogeneous embankments by S. E. Coleman, D. P. Andrews, and M. G. Webby. *Journal of Hydraulic Engineering, 130*(4), 371–376.

Coleman, S. E., Andrews, D. P., & Webby, M. G. (2002). Overtopping breaching of noncohesive homogeneous embankments. *Journal of Hydraulic Engineering, 128*(9), 829–838.

Costabile, P., Costanzo, C., & Macchione, F. (2012). Comparative analysis of overland flow models using finite volume schemes. *Journal of Hydroinformatics, 14*(1), 122-135.

Costabile, P., & Macchione, F. (2015). Enhancing river model set-up for 2-D dynamic flood modeling. *Environmental Modelling and Software, 67*, 89-107.

Costabile, P., Macchione, F., Natale, L., & Petaccia, G. (2014). *Representing skewed bridge crossing on 1-D and 2-D flood propagation models: compared analysis in practical studies. In: Schleiss, A.J., De Cesare, G., Franca, M.J., Pfister, M. (Eds.).* Paper presented at the Proceedings of the International Conference on Fluvial Hydraulics, River Flow 2014.

Costabile, P., Macchione, F., Natale, L., & Petaccia, G. (2015). Flood mapping using LIDAR DEM. Limitations of the 1-D modeling highlighted by the 2-D approach. *Natural Hazards, 77*, 181-204.

Costabile, P., Macchione, F., & Rinaldi, L. (2004). *Schema monodimensionale per il calcolo dell'erosione di rilevati in materiale sciolto.* Paper presented at the Proc., 29th Convegno di Idraulica e Costruzioni Idrauliche, Cosenza, Italy.

Cunge, J. A., Holly, F. M., Jr, & Verwey, A. (1980). Practical aspects of computational river hydraulics. Boston: Pitman Advanced Publishing Program.

De Lorenzo, G., & Macchione, F. (2010). *Numerical simulations of some dam breach experimental tests.* Paper presented at the In Proceedings of the First European IAHR Congress, Edinburgh, Scotland.

De Lorenzo, G., & Macchione, F. (2011). Capability of a numerical model to simulate dam breach laboratory tests. *Journal of Flood Risk Management, 4*, 298–305.

De Lorenzo, G., & Macchione, F. (2014). Formulae for the Peak Discharge from Breached Earthfill Dams. *Journal of Hydraulic Engineering, 140*, 56–67.

Demir, I., & Krajewksi, W. F. (2013). Towards an integrated Flood Information System: Centralized data access, analysis, and visualization. *Environmental Modelling & Software, 50*, 77-84.

Duricic, J., Erdik, T., & van Gelder, P. (2013). Predicting peak discharge due to embankment dam failure. *Journal of Hydroinformatics, 15*(4), 1361-1376.

Faeh, R. (2007). Numerical Modelling of Breach Erosion of River Embankments. *Journal of Hydraulic Engineering, 133*(9), 1000-1009.

FLDWAV, N. (1998). NWS FLDWAV MODEL: THEORETICAL DESCRIPTION by D.L. Fread USER DOCUMENTATION by J.M. Lewis. Retrieved November 28, 1988, from http://www.rivermechanics.net/models/fldwav_doc.pdf

Franca, M. J., & Almeida, A. B. (2004). A computational model of rockfill dam breaching caused by overtopping (RoDaB). *Journal of Hydraulic Research, 42*(2), 197-206.

Fread, D. L. (1988a). BREACH: An erosion model for earthen dam failures *U.S. National Weather Service Report*. Silver Spring, Md.

Fread, D. L. (1988b). "The NWS DAMBRK model: Theoretical background/user documentation." HRL-258. Silver Spring, Md: Hydrologic Research Laboratory Report, National Weather Service.

Fread, D. L. (1989). National weather service models to forecast dam breach floods. *Hydrology of disasters*, 192-211.

Fread, D. L., & Harbaugh, T. E. (1973). Transient hydraulic simulation of breached earth dams. *Journal of Hydraulic Division, 99*(1), 139-154.

Froehlich, D. C. (1995a). *Embankment dam breach parameters revisited.* Paper presented at the Proceedings of the 1995 ASCE Conference on Water Resources Engineering, San Antonio, Texas.

Froehlich, D. C. (1995b). Peak outflow from breached embankment dams. *Journal of Water Resources Planning and Managemen, 121*(1), 90-97.

Froehlich, D. C. (2002, september). *Impact project field tests 1 and 2: "blind" simulation by Davef.* Paper presented at the Proceedings of 2nd IMPACT Project Workshop: Mo-i-Rana, Norway.

Giuseppetti, G., & Molinaro, P. (1989). *A mathematical model of the erosion of an embankment dam by overtopping.* Paper presented at the Proc., Int. Symp. on Analytical Evaluation of Dam Related Safety Problems, Copenhagen, Denmark.

Hanson, G. J., Cook, K. R., & Hunt, S. L. (2005). Physical modelling of overtopping erosion and breach formation of cohesive embankments. *Transaction of the ASAE, 48*, 1783-1794.

Hassan, M. A. A. M., Samuels, P. G., Morris, M. W., & Ghataora, G. S. (2002). *Improving the accuracy of predictions of breach formation through embankment dams and flood embankments.* Paper presented at the Int. Conf. On Fluvial Hydraulics (4.-6. Sept), Louvain-la-Neuve. Belgium.

IMPACT. (2005). Investigation of Extreme Flood Process and Uncertainty *WP2 publications—Technical reports "Baldwin Hills Dam failure." Civ. Eng.*

Johnson, F. A., & Illes, P. (1976). A classification of dam failures. *Int. Water Power Dam Constr, 28*(12), 43 – 45.

Liang, Q., & Smith, L. S. (2015). A high-performance integrated hydrodynamic modelling system for urban flood simulations. *Journal of Hydroinformatics, 17*(4), 518-533.

Loukola, E., & Huokona, M. (1998, 8-9 October). *A numerical erosion model for embankment dams failure and its use for risk assessment.* Paper presented at the In proceedings of "CADAM (Concerted Action on Dam Break Modelling)", Munich Meeting.

Macchione, F. (1986). Sull'idrogramma di piena conseguente alla rottura degli sbarramenti in materiali sciolti. *Memoria Interna, 139*.

Macchione, F. (1989). Discussion on: Dimensionless analytical solution for dam breach erosion. *Journal of Hydraulic Research, 27*(2), 447-452.

Macchione, F. (1993). *Alluvioni artificiali conseguenti a rotture di dighe.* Paper presented at the Fenomeni alluvionali artificiali a valle delle dighe, Cosenza, Italy.

Macchione, F. (2000). *Le piene derivanti dall'erosione degli sbarramenti in materiali sciolti.* Paper presented at the Sistemazione dei corsi d'acqua, Cosenza, Italy.

Macchione, F. (2008). Model for Predicting Floods due to Earthen Dam Breaching. I: Formulation and Evaluation. *Journal of Hydraulic Engineering, 134*(12), 1688-1696.

Macchione, F., Costabile, P., Costanzo, C., & Razdar, B. (2015a). Dam breach modelling: influence on downstream water levels and a proposal of a physically based module for flood propagation software. *Journal of Hydroinformatics* (Accepted).

Macchione, F., Costabile, P., Costanzo, C., & Razdar, B. (2015b). *Ricostruzione numerica dell'evento di piena generato dalla rottura della diga di Big Bay, USA.* Paper presented at the atti del 36° Corso di Aggiornamento in Tecniche per la Difesa dall'Inquinamento, Guardia Piemontese, 17-20 Giugno 2015, Edibios (CS).

Macchione, F., De Lorenzo, G., Costabile, P., & Razdar, B. (2015). The power function for representing the reservoir rating curve: morphological meaning and suitability for dam breach modeling. *Water Resources Management* (under review).

Macchione, F., & Rino, A. (2008). Model for Predicting Floods due to Earthen Dam Breaching. II: Comparison with Other Methods and Predictive Use. *Journal of Hydraulic Engineering, 134*(12), 1697-1707.

Macchione, F., & Sirangelo, B. (1989). *Study of earth dam erosion due to overtopping.* Paper presented at the Hydrology of disasters, London.

Macchione, F., & Sirangelo, B. (1990). *Floods resulting from progressively breached dams.* Paper presented at the In Proceedings of Hydrology in Mountainous regions II - Artificial Reservoirs, Water and Slopes.

MacDonald, T. C., & Langridge-Monopolis, J. (1984). Breaching Characteristics of Dam Failures. *Journal of Hydraulic Engineering, 110*(5), 567-586.

Marone, V. (1971). Calcolo di massima di un serbatoio di laminazione. *Energia Elettrica, 48*, 561-567.

Michels, V. M. (1977). Reservoir basin morphometry. *Journal of the Irrigation and Drainage Division, 103*, 13-31.

Mohamed, M. A. A., Samuels, P. G., Morris, M. W., & Gathaora, G. S. (2002). *Improving the accuracy of predictions of breach formation through embankment dams and flood embankments.* Paper presented at the River Flow 2002, Proc., Int. Conf. on Fluvial Hydraulics, Balkema, Liss, The Netherlands.

Mohammadzadeh-Habili, J., Heidarpour, M., Mousavi, S., & Haghiabi, A. H. (2009). Derivation of reservoir's area-capacity equations. *Journal of Hydrologic Engineering, 14*, 1017–1023.

Morris, M. W., Hanson, G. J., & Hassan, M. (2008). Improving the accuracy of dam breach modelling: why are not we progressing faster? *Journal of Flood Risk Management, 1*, 150-161.

Peng , M., & Zhang, L. M. (2012). Breaching parameters of landslide dams. *Landslides, 9*(1), 13-31.

Peviani, M. (1999, 18-19 November, 1999.). *Simulation of earth-dams breaking processes by means of a morphological numerical model.* Paper presented at the In proceedings of "CADAM (Concerted Action on Dam Break Modelling)", Zaragoza.

Pierce, M. W., Thornton, C. I., & Abt, S. R. (2010). Predicting breach outflow from breached embankment dams. *Journal of Hydrologic Engineering, 15*(5), 338-349.

Ponce, V. M., & Tsivoglou, A. J. (1981). Modeling gradual dam breaches. *Journal of Hydraulic Division ASCE, 107*, 829-838.

Qi, H., & Altinakar, M. S. (2011). A GIS-based decision support system for integrated flood management under uncertainty with two dimensional numerical simulations. *Environmental Modelling & Software, 26*, 817-821.

Rozov, A. L. (2003). Modeling of washout of dams. *Journal of Hydraulic Research, 41*(6), 565-577.

Ruiz-Villanueva, V., Bladé, E., Sánchez-Juny, M., Marti-Cardona, B., Díez-Herrero, A., & Bodoque, J. M. (2014). Two-dimensional numerical modeling of wood transport. *Journal of Hydroinformatics, 16*(5), 1077-1096.

Russo, B., Sunyer, D., Velasco, M., & Djordjević, S. (2015). Analysis of extreme flooding events through a calibrated 1D/2D coupled model: the case of Barcelona (Spain). *Journal of Hydroinformatics, 17*(3), 473-491.

Singh, K. P., & Snorasson, A. (1984). Sensitivity of outflow peaks and flood stages to the selection of dam breach parameters and simulation models. *Journal of Hydrology, 68*, 295-310.

Singh, V. P. (1996). *Dam breach modeling technology*. Norwell, Massachusetts: Kluwer Academic.

Singh, V. P., & Quiroga, C. A. (1987). A dam-breach erosion model: I. formulation. *Water Resources ManagemenT, 1*, 177-197.

Singh, V. P., & Quiroga, C. A. (1988). Dimensionless analytical solution for dam breach erosion. *Journal of Hydraulic Research, 26*(2), 179-197.

Singh, V. P., & Scarlatos, P. D. (1988). Analysis of Gradual Earth-Dam Failure. *Journal of Hydraulic Engineering, 114*(2), 21-42.

Singh, V. P., & Scarlatos, P. D. (1989). Breach erosion of earthfill dams and flood routing: BEED model (E. Laboratory, Trans.). In M. P. EL-79-6 (Ed.), *Military Hydrology Rep*. Vicksburg, Miss.

Tinney, E. R., & Hsu, Y. H. (1961). Mechanics of washout of an erodible fuse plug. *Journal of Hydraulic Division, 87*, 1-29.

Tsakiris, G., & Spiliotis, M. (2013). Dam-breach hydrograph modelling: An innovative semi-analytical approach. *Water Resources ManagemenT, 27*, 1751-1762.

Visser, P. J. (1998). Breach growth in sand-dikes: Ph.D. thesis Delft University of Technology.

Vojinovic, Z., Seyoum, S., H, S. M., Price, R. K., Fikri, A. K., & Abebe, Y. (2013). Modelling floods in urban areas and representation of buildings with a method based on adjusted conveyance and storage characteristics. *Journal of Hydroinformatics, 15*(4), 1150-1168.

Wahl, T. L. (1998). Prediction of embankment dam breach parameters - A literature review and needs assessment. Denver: U. S. Department of Interior - Bureau of Reclamation.

Wahl, T. L. (2004). Uncertainty of Predictions of Embankment Dam Breach Parameters. *Journal of Hydraulic Engineering, 130*(5), 389-397.

Walder, J. S., & O'Connor, J. E. (1997). Methods for predicting peak discharge of floods caused by failure of natural and constructed earthen dams. *Water Resources Research, 33*(10), 2337-2348.

Wang, Z., & Bowles, D. (2006a). Three-dimensional non-cohesive earthen dam breach model. part 1: Theory and methodology. *Advances in Water Resources, 29*, 1528-1545.

Weiming, W. (2013). Simplified Physically Based Model of Earthen Embankment Breaching. *Journal of Hydraulic Engineering, 139*(8), 837-851.

Xu, Y., & Zhang, M. (2009). Breaching parameters for earthfill and rockfill dams. *Journal of Geotechnical and Geoenvironmental Engineering, 135*(12), 1957-1970.

Yochum, S. E., Goertz, L. A., & Jones, P. H. (2008). Case Study of the Big Bay Dam Failure: Accuracy and Comparison of Breach Predictions. *Journal of Hydraulic Engineering, 134*(9), 1285-1293.